recycling

MDPI

Article

Improving the Performance of Recycled Multilayer PET Through Reactive Compatibilization Strategies

Aritz Unamuno Garay [1], Fernando Galera Pérez [1], Ana Ibáñez-García [2], Asunción Martínez-García [2] and María Dolores Samper [1,*]

[1] Instituto Universitario de Tecnología de Materiales, Universitat Politècnica de València, Plaza Ferrándiz y Carbonell s/n, 03801 Alcoy, Spain; aunagar@upv.edu.es (A.U.G.); fgalper@epsa.upv.es (F.G.P.)
[2] AIJU Instituto Tecnológico de Producto Infantil y Ocio, Avda. de la Industria, 23, 03440 Ibi, Spain; anaibanyez@aiju.es (A.I.-G.); sunymartinez@aiju.es (A.M.-G.)
* Correspondence: masammad@upv.es

Abstract

The recycling of post-industrial multilayer polyethylene terephthalate (mPET) packaging waste remains a major challenge due to the coexistence of incompatible polymeric phases and the deterioration of properties during reprocessing. In this work, different reactive compatibilization strategies were evaluated to improve the processability and performance of recycled multilayer PET scraps generated during industrial packaging manufacturing processes. Several functional compatibilizers were investigated, including poly(ethylene-co-acrylic acid) (EAA), poly(ethylene-alt-maleic anhydride) (EMA), poly(ethylene-co-glycidyl methacrylate) (EGMA), poly(ethylene-co-methyl acrylate-co-glycidyl methacrylate) (EMAGMA), and maleic anhydride (MA). The influence of compatibilization on the thermal, mechanical, chemical, surface, and morphological properties of recycled mPET was systematically analyzed. Processing behavior revealed that EMA- and MA-based formulations could not be successfully injection molded. In contrast, EAA-, EGMA-, and EMAGMA-based formulations showed suitable processability and enabled the production of defect-free specimens. Thermogravimetric analysis revealed only minor changes in thermal degradation behavior after compatibilization. In contrast, differential scanning calorimetry revealed changes in the melting behavior of the recycled formulations, while tensile and impact tests demonstrated marked improvements in ductility and toughness for EGMA- and EMAGMA-modified systems. Among them, EMAGMA provided the highest elongation at break and impact resistance. Contact angle measurements showed moderate changes in surface wettability, whereas density and hardness remained largely unaffected. FESEM analysis revealed a more homogeneous phase distribution and reduced dispersed-domain size in the compatibilized formulations, particularly for EGMA, indicating improved interfacial compatibility. These results demonstrate that glycidyl methacrylate-based compatibilizers are effective reactive agents for upgrading post-industrial multilayer PET waste into higher-performance recycled materials for different applications.

Keywords: multilayer PET; reactive compatibilization; circular economy

Check for updates

Academic Editor: Denis Rodrigue

Received: 30 June 2026
Revised: 30 July 2026
Accepted: 1 August 2026
Published: 7 August 2026

Copyright: © 2026 by the authors. Licensee MDPI, Basel, Switzerland. This article is an open access article distributed under the terms and conditions of the Creative Commons Attribution (CC BY) license.

1. Introduction

The growing use of plastic materials in food and industrial packaging has raised significant environmental concerns due to the continuous accumulation of plastic waste

and the limited recyclability of complex polymer systems. In particular, multilayer plastic packaging has become widely adopted because it combines different polymeric materials within a single structure, providing tailored properties such as mechanical strength, flexibility, thermal stability, transparency, and excellent barrier properties against oxygen and moisture. These systems typically consist of polymers such as polyethylene terephthalate (PET), polyethylene (PE), polypropylene (PP), polyamide (PA), and ethylene vinyl alcohol (EVOH), where each component contributes specific functional properties. For instance, PET provides stiffness and transparency, PE contributes flexibility and sealability, while PA and EVOH enhance gas barrier performance.

Despite these advantages, multilayer structures present significant end-of-life challenges due to the intrinsic immiscibility of their constituent polymers and the difficulty of separating them using conventional recycling routes. During mechanical recycling, these incompatibilities lead to phase separation, poor interfacial adhesion, and heterogeneous morphologies, resulting in materials with reduced mechanical performance, reduced ductility, and limited opportunities for high-value applications [1,2]. As reported in recent studies, multilayer packaging waste is often discarded or downcycled because mechanical recycling processes are unable to preserve the required material quality [3,4].

Mechanical recycling remains the most widely applied and economically attractive option for polymer waste management due to its lower energy consumption and infrastructure requirements compared with chemical recycling routes. However, its effectiveness is significantly reduced when dealing with mixed or multilayer waste streams. In this context, alternative strategies such as compatibilization, selective dissolution–precipitation, delamination, and chemical depolymerization have been extensively investigated to improve the valorization of complex plastic waste [4–7].

Among these alternatives, chemical recycling technologies, such as hydrolysis, glycolysis and enzymatic depolymerization, have demonstrated considerable potential for recovering valuable monomers from PET-containing multilayer structures. These approaches enable the production of high-purity compounds such as terephthalic acid (TPA) and bis(2-hydroxyethyl) terephthalate (BHET), which can be reintroduced into the polymer value chain [4,8,9]. Nevertheless, despite their technical advantages, these processes often require additional separation, purification, and chemical processing steps, which may limit their economic viability when compared to mechanical recycling.

Multilayer PET (mPET) structures are increasingly used in food packaging applications, particularly in thermoformed trays and barrier packaging, due to their excellent combination of stiffness, transparency, processability, and barrier performance. However, the presence of polyolefin and barrier layers compromises the quality of mechanically recycled PET, making effective compatibilization strategies essential for obtaining recycled materials with acceptable performance.

Alongside chemical recycling approaches, compatibilization has been widely studied as a mechanical strategy to improve the recyclability of immiscible polymer blends. Maleic anhydride (MA)-based compatibilizers, such as polyethylene-grafted maleic anhydride (PE-g-MA), are among the most commonly used additives for improving the compatibility of immiscible polymer blends by enhancing interfacial interactions and reducing phase separation between polar and non-polar phases [10–14]. Glycidyl methacrylate-based compatibilizers, such as ethylene-glycidyl methacrylate (EGMA), have also demonstrated considerable improvements in impact resistance and toughness in blends of PET and polyolefins [10,13–17]. Commercial systems such as DuPont Fusabond® and Dow RETAIN® have further proven the industrial relevance of compatibilization technologies in improving phase dispersion and enabling the recycling of multilayer barrier films containing EVOH, PA, and PE.

Other studies have shown that the incorporation of reactive compatibilizers can improve the recyclability of multilayer polymer systems by enhancing interfacial interactions, mechanical performance, and processability of the recycled blends [10,11,15,18,19]. Nevertheless, even with compatibilization, the immiscibility of certain polymer combinations (e.g., PE/PA or PET/PE systems) continues to limit the achievable performance of recycled materials, particularly when the multilayer composition is highly complex or variable [10,11,15].

Post-industrial multilayer PET scraps generated during packaging manufacturing represent an attractive feedstock for recycling because they are available in large volumes and exhibit lower contamination levels than post-consumer waste. However, despite their higher purity, the heterogeneous multilayer structure still limits their direct reprocessing and requires effective compatibilization strategies to achieve high-quality recycled materials.

Despite the significant progress achieved in both mechanical and chemical recycling technologies, the efficient valorization of recycled multilayer PET systems remains a major challenge. The final performance of recycled materials strongly depends on compatibilizer chemistry, compatibilizer concentration, processing conditions, and resulting phase morphology [10,20]. Moreover, chemical recycling routes must balance conversion efficiency, selectivity, and economic feasibility, particularly when applied to heterogeneous real-world waste streams.

In this context, recent literature has emphasized the need for integrated recycling strategies combining mechanical, physical, and chemical approaches to maximize material recovery from multilayer packaging waste [3,4]. The development of scalable and robust processes capable of handling real post-consumer waste remains essential to advance toward a circular economy for plastics.

Although several studies have investigated the compatibilization of multilayer polyolefin systems and PET/polyolefin blends [10,13], comparative information regarding the effectiveness of different reactive compatibilizers in post-industrial multilayer PET waste remains limited. In particular, the influence of maleic anhydride- and glycidyl methacrylate-based compatibilizers on the thermal, mechanical, surface, and morphological properties of recycled mPET has not been comprehensively evaluated.

Therefore, the aim of this work was to evaluate the effectiveness of different reactive compatibilization strategies for the recycling of post-industrial multilayer PET scraps generated during packaging manufacturing. Several compatibilizers, including EAA, EMA, MA, EGMA, and EMAGMA, were incorporated through melt blending at different concentrations. The resulting materials were characterized by differential scanning calorimetry (DSC), thermogravimetric analysis (TGA), Fourier transform infrared spectroscopy (FTIR), contact angle measurements, field-emission scanning electron microscopy (FESEM), and mechanical testing in order to establish structure–property relationships and identify the most suitable compatibilization strategy for improving the processability and performance of recycled mPET.

2. Results

2.1. Characterization mPET Residue

2.1.1. Size and Distribution of mPET Flakes

Figure 1 shows the post-industrial multilayer mPET flakes used as the starting material in this study. The residue consisted of irregular transparent flakes obtained from mechanically shredded industrial edge trims.

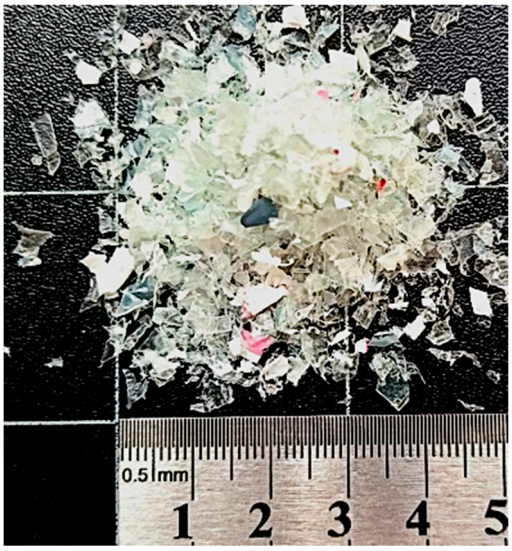


Figure 1. Photograph of the post-industrial multilayer mPET flakes used as feedstock.

From the particle size distribution graph (Figure 2), most mPET flakes were concentrated in the 1–2 mm size range. The fraction retained on the 2 mm sieve was the predominant one, accounting for approximately 51% of the sample, followed by the fraction retained on the 1 mm sieve, which represented about 35%. Together, these two fractions accounted for approximately 86% of the analyzed material, indicating a relatively homogeneous particle-size distribution concentrated in the smaller size range.

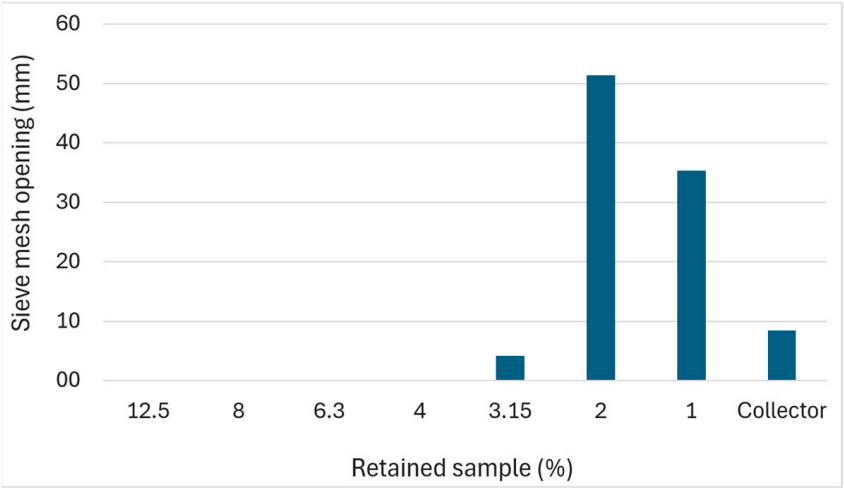


Figure 2. Distribution particle size of the mPET flakes residue.

2.1.2. Bulk Density

The experimentally determined bulk density of the mPET waste was 0.174 ± 0.003 g/mL, reflecting the loose packing arrangement of the material in its as-received condition. Such a low bulk density is typical of shredded or flake-shaped plastic waste, where significant interparticle voids result in a high volume-to-mass ratio. From a processing perspective, this characteristic has important implications for material handling, storage, transportation, and feeding operations. Although the relatively narrow particle-size distribution contributes to a more homogeneous melting behavior during extrusion, the irregular geometry and low bulk density of the flakes may reduce feeding efficiency in conventional gravity-fed hoppers because of particle bridging and void formation. Consequently, industrial-scale

processing of this type of residue would benefit from the use of forced-feeding or crammer feeder systems to ensure a continuous and stable material flow into the extruder.

2.1.3. Moisture Content

The moisture content of the post-industrial multilayer mPET residue, Table 1, determined according to the gravimetric procedure described in Section 4.2.3, was 0.52 ± 0.03 wt.%. Drying the flakes under the processing conditions adopted in this work (40 °C for 24 h) resulted in a mass loss of 0.27 ± 0.02 wt.%, corresponding to approximately half of the total moisture determined by the standard gravimetric procedure.

Table 1. Effect of drying conditions on the mass loss of the post-industrial multilayer mPET residue.

Drying Condition	Mass Loss (wt.%)
40 °C—24 h	0.273 ± 0.022
105 °C—4 h	0.524 ± 0.049
105 °C—24 h	0.517 ± 0.029

Although drying at 105 °C for 4 h and 24 h produced similar mass losses (0.52 ± 0.05 and 0.52 ± 0.03 wt.%, respectively), indicating that moisture removal was essentially complete after 4 h, preliminary observations revealed that exposure to this temperature induced slight curvature of the multilayer flakes together with partial adhesion between adjacent particles. Although drying at around 105 °C is commonly employed for conventional PET materials, the heterogeneous nature of the multilayer residue used in this study made it more susceptible to these physical changes. In contrast, drying at 40 °C for 24 h preserved the original flake morphology, facilitating subsequent handling and feeding during extrusion. For this reason, the lower drying temperature was selected as a compromise between moisture removal and preservation of the physical integrity of the heterogeneous multilayer feedstock.

Despite the lower moisture removal achieved at 40 °C, no processing defects associated with residual moisture, such as bubble formation, vapor evolution, or unstable melt flow, were observed during reactive extrusion or injection molding. These observations indicate that the selected drying conditions were sufficient to ensure stable processing while avoiding the physical changes induced by drying at higher temperatures.

2.2. Mechanical Characterization

2.2.1. Tensile Properties

The incorporation of reactive compatibilizers into the recycled multilayer PET (mPET) matrix produced significant modifications in the tensile behavior of the material, particularly in terms of tensile strength, Young's modulus, and elongation at break. The results demonstrate that the compatibilization strategy strongly influences the balance between stiffness, toughness, and ductility of the recycled polymer blends, as shown in Figure 3. In addition to the conventional tensile parameters, the representative stress–strain curves (Figure 3d) provide further insight into the deformation behavior of the compatibilized systems, allowing the evolution of the plastic deformation region to be directly visualized.

The incorporation of ethylene-glycidyl methacrylate (EGMA) produced a considerably more favorable mechanical response. At low concentrations (1–2 phr), EGMA caused a reduction in tensile strength to values around 39 MPa, representing a decrease of approximately 15% compared with the reference mPET. However, increasing the EGMA concentration progressively restored the tensile strength, with formulations containing 3 phr or more exhibiting values comparable to those of the unmodified material. Although some differences fell within the experimental variability, the overall trend suggests that

increasing the EGMA concentration promotes more effective interactions between the different phases present in the heterogeneous multilayer structure, facilitating more efficient stress transfer during tensile deformation.

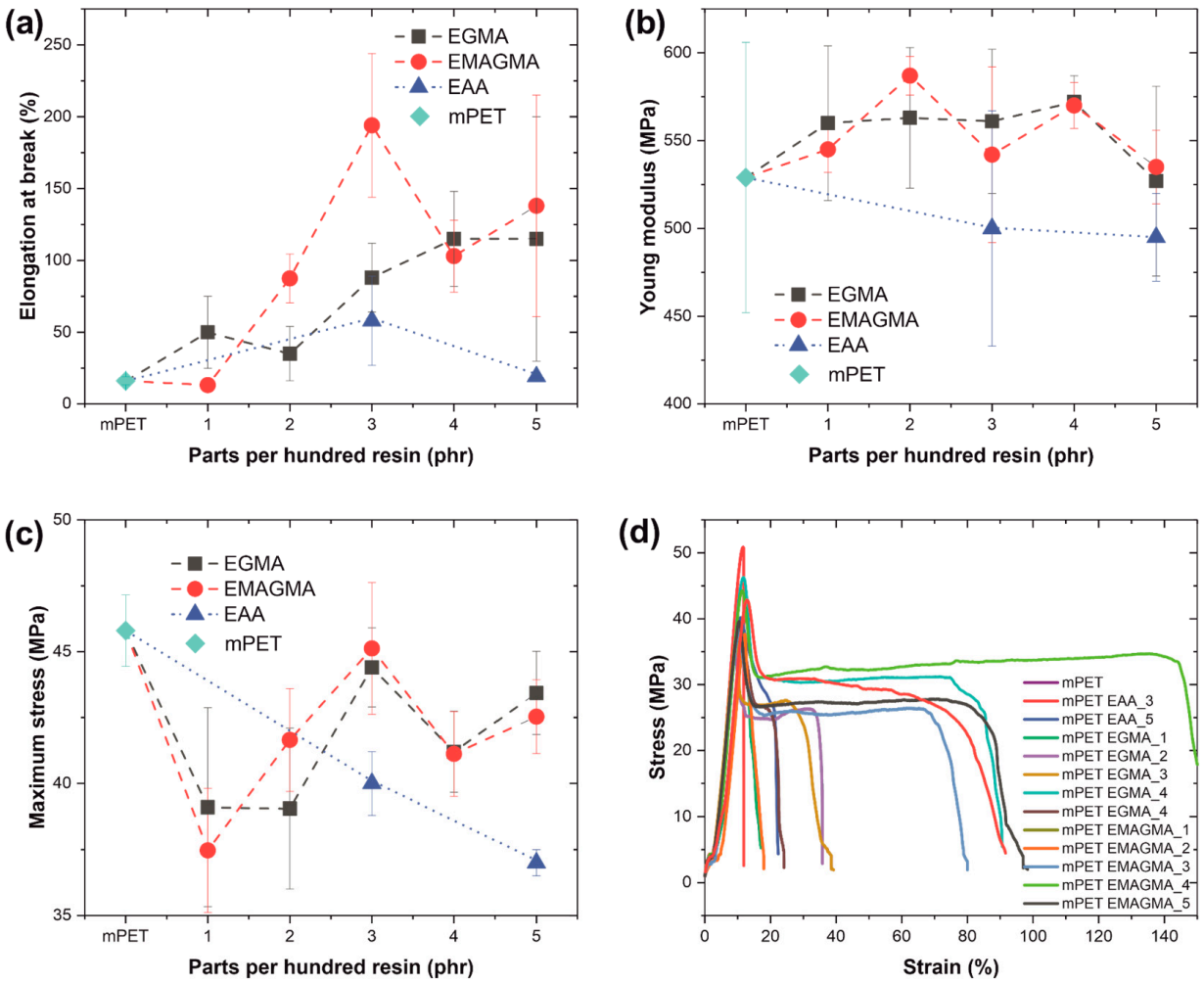


Figure 3. Effect of compatibilizer content on the tensile properties of recycled multilayer PET formulations: (**a**) elongation at break, (**b**) Young's modulus, (**c**) tensile strength, and (**d**) representative stress–strain curves. Error bars represent the standard deviation.

In addition to the retention of tensile strength, EGMA significantly enhanced the ductility of the recycled material. The elongation at break increased progressively with compatibilizer concentration, reaching values of 88% for EGMA_3 and exceeding 115% for both EGMA_4 and EGMA_5. This progressive improvement is also clearly reflected in the representative stress–strain curves (Figure 3d), where the EGMA-containing formulations exhibit a substantial extension of the plastic deformation region compared with the unmodified mPET. This marked increase in elongation at break suggests that EGMA effectively improves the deformability of the recycled material while maintaining adequate tensile strength.

Regarding stiffness, the Young's modulus of the EGMA formulations remained close to that of the reference mPET (529 ± 77 MPa), with values ranging from 527 ± 54 to 572 ± 15 MPa. The relatively small variations observed indicate that EGMA improves ductility without substantially compromising the stiffness of the recycled material. In particular, EGMA_4 exhibited the highest modulus within this series (572 ± 15 MPa), suggesting that effective compatibilization can be achieved while preserving structural stiffness.

The relatively large standard deviations observed for some formulations may be associated with the heterogeneous nature of the recycled multilayer feedstock, which can lead to local variations in phase distribution and interfacial interactions. Consequently, while clear trends can be identified, some differences between individual formulations should be interpreted considering the experimental variability.

Among all the compatibilizers evaluated, ethylene-methyl acrylate-glycidyl methacrylate (EMAGMA) exhibited the most remarkable effect on tensile ductility. Similar to EGMA, low concentrations of EMAGMA slightly reduced the tensile strength of the recycled material, with values close to 39 MPa for EMAGMA_1 and EMAGMA_2. However, the formulation containing 3 phr EMAGMA exhibited a tensile strength of 45.12 MPa, practically identical to the reference mPET, indicating excellent retention of tensile strength and an effective modification of the heterogeneous multilayer structure. More importantly, EMAGMA produced the highest elongation at break among all the investigated compatibilizers, reaching values close to 200% at 3 phr. This remarkable improvement is clearly evidenced by the stress–strain curves (Figure 3d), where the EMAGMA formulations displayed the widest plastic deformation region while maintaining tensile strength values comparable to those of the reference material. This exceptional increase suggests that EMAGMA provides a more effective modification of the heterogeneous multilayer structure, resulting in enhanced deformation capability and energy absorption during tensile loading.

The EMAGMA_4 and EMAGMA_5 formulations also exhibited high elongation at break values compared with the reference material, confirming the positive effect of this compatibilizer on ductility over a relatively broad concentration range. Although the maximum elongation was obtained for EMAGMA_3, the consistently high ductility observed for the remaining EMAGMA formulations indicates that this compatibilizer provides an effective balance between strength and deformability over a relatively wide concentration window.

The Young's modulus results further support the effectiveness of EMAGMA as a compatibilizer. The modulus values ranged from 535 $\pm$ 21 to 587 $\pm$ 11 MPa, remaining comparable to or slightly higher than that of the reference mPET. The highest value was obtained for EMAGMA_2 (587 $\pm$ 11 MPa), while several formulations exhibited remarkably low standard deviations, indicating good reproducibility of the mechanical response. Overall, the Young's modulus remained within the same range as that of the reference material, demonstrating that the remarkable increase in ductility was achieved without an appreciable loss of stiffness.

The improvement in toughness obtained with EMAGMA is particularly relevant considering the intrinsic recycling difficulties associated with multilayer PET waste. Previous studies have shown that multilayer PET structures generally exhibit poor recyclability because the coexistence of incompatible phases generates weak interfaces and heterogeneous morphologies [10,11]. Therefore, the substantial increase in elongation at break observed in the present work highlights the potential of reactive compatibilization as an effective strategy for improving the performance of recycled multilayer packaging waste.

EAA showed a different behavior compared to the other compatibilizers. Although the EAA-containing formulations maintained acceptable tensile strength values, a gradual decrease was observed with increasing compatibilizer concentration. Tensile strength values of 40.40 MPa and 37.40 MPa were obtained for EAA_3 and EAA_5, respectively, implying a more significant loss in mechanical strength compared to EGMA and EMAGMA. Regarding elongation at break, EAA_3 exhibited an increase to approximately 58%, indicating an improvement in ductility compared with the reference mPET. However, the EAA_5 formulation showed a substantial reduction in elongation at break, reaching only 19%. The

representative stress–strain curves (Figure 3d) further support this behavior, revealing only a limited extension of the plastic deformation region for the EAA formulations, particularly at the highest compatibilizer concentration. This behavior suggests that increasing the EAA concentration beyond a certain level does not provide additional compatibilization benefits and may negatively affect the deformation capability of the recycled material.

A similar trend was observed for Young's modulus. The EAA formulations exhibited values of approximately 500 ± 67 MPa and 495 ± 25 MPa, slightly lower than the reference mPET. This reduction in stiffness is consistent with the decrease in tensile strength and suggests that EAA is less effective than EGMA and EMAGMA in preserving the mechanical integrity of the recycled multilayer structure.

Among the three compatibilizers, EMAGMA exhibited the most significant improvement in ductility while maintaining tensile strength values comparable to those of the reference material. EGMA also produced a progressive increase in ductility while preserving Young's modulus and recovering tensile strength at compatibilizer contents of 3 phr and above. In contrast, EAA showed a more limited ability to improve the tensile performance of the recycled multilayer system.

Interestingly, the compatibilizers that exhibited the best processability during injection molding (EGMA and EMAGMA) were also those that provided the greatest improvements in tensile ductility. Furthermore, these formulations exhibited the largest extension of the plastic deformation region in the stress–strain curves, indicating a more efficient redistribution of deformation before failure. This correlation suggests that improved processability and enhanced mechanical performance may originate from improved phase dispersion within the heterogeneous multilayer structure.

This behavior is consistent with previous studies on the reactive compatibilization of multilayer polymer systems. Moreno and Saron reported that maleic anhydride-grafted compatibilizers improve the mechanical performance of immiscible polymer blends by enhancing interactions between phases and reducing phase separation phenomena during melt processing [10]. Similarly, Turriziani et al. observed that reactive compatibilizers incorporated into multilayer packaging structures improve tensile stress transfer and facilitate the mechanical recycling of complex polymer systems [11]. The trends observed in the present work are consistent with these studies, since the compatibilizers exhibiting the best overall mechanical performance (EGMA and EMAGMA) also produced the most pronounced increase in ductility while maintaining tensile strength and stiffness at levels comparable to those of the reference material. The remarkable increase in elongation at break observed for the EGMA and EMAGMA formulations is in agreement with previous reports describing the effectiveness of reactive compatibilizers in improving the mechanical performance of recycled multilayer materials through enhanced phase compatibility and reduced stress concentration effects.

2.2.2. Charpy Impact Testing and Shore D Hardness

The Charpy impact results confirmed the trends observed during tensile testing and provided additional information regarding the toughness and energy absorption capacity of the compatibilized formulations, as shown in Table 2.

The incorporation of EAA, EGMA, and EMAGMA into mPET has distinct effects on impact strength, showing different trends depending on the compatibilizer chemistry.

The addition of EAA produced only limited changes in impact resistance compared with the reference mPET, which had an impact strength of 2.4 kJ/m^2, while mPET EAA_3 (2.45 kJ/m^2) and mPET EAA_5 (2.50 kJ/m^2) showed minor decreases of 10–12%. This suggests that EAA does not significantly enhance toughness and might slightly weaken the polymer's resistance to impact, likely due to its softening effect without substantial

energy dissipation improvements. In contrast, EGMA progressively improved the impact strength as the compatibilizer concentration increased. Although the EGMA_1 formulation showed impact strength values similar to those of the reference material, higher EGMA concentrations resulted in a gradual increase in impact resistance, reaching 3.51 kJ/m^2 for EGMA_4 and 3.40 kJ/m^2 for EGMA_5. These results represent an increase of approximately 27% compared with unmodified mPET. The increase in impact strength observed for the EGMA formulations is consistent with the improvements in elongation at break previously reported during tensile testing, suggesting a more effective toughening of the recycled multilayer structure.

Table 2. Charpy impact strength and Shore D hardness of the recycled mPET formulations modified with EAA, EGMA, and EMAGMA. Values are reported as mean ± standard deviation.

Sample	Charpy Impact Strength (kJ/m^2)	Shore D Hardness
mPET	2.4 ± 1.0	73.0 ± 1.0
mPET EAA_3	2.5 ± 0.3	72.8 ± 0.8
mPET EAA_5	2.5 ± 0.5	71.2 ± 0.8
mPET EGMA_1	2.6 ± 0.5	70.7 ± 1.2
mPET EGMA_2	3.0 ± 0.5	71.0 ± 0.8
mPET EGMA_3	3.1 ± 0.3	73.6 ± 0.5
mPET EGMA_4	3.5 ± 0.5	70.0 ± 0.8
mPET EGMA_5	3.4 ± 0.5	72.8 ± 0.4
mPET EMAGMA_1	2.4 ± 0.2	71.7 ± 1.2
mPET EMAGMA_2	3.0 ± 0.1	70.7 ± 1.0
mPET EMAGMA_3	3.7 ± 0.1	73.0 ± 0.7
mPET EMAGMA_4	3.5 ± 0.6	70.7 ± 0.8
mPET EMAGMA_5	5.5 ± 0.3	73.2 ± 0.8

The most significant improvement in impact performance was achieved with EMAGMA. While the EMAGMA_1 formulation exhibited impact strength values comparable to those of the reference material, increasing compatibilizer concentrations generated substantial improvements in toughness. The impact strength reached 3.75 kJ/m^2 for EMAGMA_3 and 5.50 kJ/m^2 for EMAGMA_5, corresponding to an increase of approximately 100% relative to the reference mPET. These results demonstrate the outstanding ability of EMAGMA to enhance the impact energy absorption capacity of the recycled multilayer material. Furthermore, the remarkable increase in impact strength is consistent with the high elongation at break values observed during tensile testing, indicating that both properties are strongly correlated.

The superior performance of EMAGMA compared with EAA and EGMA suggests that this compatibilizer is more effective in promoting the mechanical integrity of the heterogeneous multilayer structure. Although the specific mechanisms responsible for this behavior will be further discussed based on the morphological and spectroscopic analyses, the mechanical results clearly indicate that EMAGMA provides the most effective toughening strategy among the compatibilizers evaluated in this study.

Overall, the impact results confirm that reactive compatibilization can significantly improve the toughness of recycled multilayer PET systems. Among the compatibilizers investigated, EMAGMA exhibited the greatest enhancement in impact resistance, followed by EGMA, whereas EAA showed only limited effectiveness. These findings are in agreement with the tensile test results and further support the potential of glycidyl methacrylate-based compatibilizers for upgrading post-industrial multilayer PET waste.

The Shore D hardness measurements (Table 3) showed only minor variations among the different formulations, indicating that the incorporation of reactive compatibilizers did not substantially affect the surface hardness of the recycled multilayer PET system.

The reference mPET exhibited a hardness of 73 ± 1 Shore D, while all compatibilized formulations remained within a narrow range of 70.0–73.6 Shore D. Considering the low compatibilizer contents investigated (1–5 phr), these limited variations were expected and indicate that the overall rigidity of the material was largely preserved. Interestingly, despite the negligible changes in hardness, several compatibilized formulations exhibited marked improvements in tensile ductility and impact resistance, demonstrating that toughness can be enhanced without compromising the surface hardness of the recycled material.

Table 3. DSC and TGA thermal parameters of the recycled mPET formulations.

Sample	ΔH_m (PET)	$T_{5\%}$ (°C)	T_{ONSET} (°C)	T_{MAX} (°C)
mPET	13.4	390.0 ± 17.1	417.9 ± 13.3	440.1 ± 4.1
mPET EAA_3	33.6	387.2 ± 0.7	420.9 ± 0.9	448.2 ± 0.6
mPET EAA_5	30.4	385.8 ± 1.8	426.3 ± 16.3	446.4 ± 3.0
mPET EGMA_1	14.5	394.2 ± 3.6	439.1 ± 17.0	445.6 ± 7.9
mPET EGMA_2	18.1	394.8 ± 0.9	426.1 ± 10.8	441.6 ± 1.3
mPET EGMA_3	16.2	390.9 ± 0.3	420.3 ± 1.0	442.9 ± 1.3
mPET EGMA_4	17.7	388.2 ± 5.0	424.7 ± 12.3	437.1 ± 2.0
mPET EGMA_5	21.3	393.1 ± 2.6	420.9 ± 1.1	446.9 ± 1.4
mPET EMAGMA_1	18.8	390.2 ± 3.4	425.1 ± 16.1	444.2 ± 4.2
mPET EMAGMA_2	17.4	391.4 ± 1.0	418.6 ± 0.3	443.5 ± 1.1
mPET EMAGMA_3	19.2	389.7 ± 2.0	416.2 ± 0.8	439.2 ± 2.8
mPET EMAGMA_4	16.7	391.1 ± 2.8	420.0 ± 1.3	447.0 ± 2.1
mPET EMAGMA_5	20.2	395.2 ± 3.6	425.3 ± 8.4	442.4 ± 3.0

2.3. Thermal Characterization

2.3.1. Differential Scanning Calorimetry (DSC)

The DSC analysis provided valuable information regarding the thermal transitions and crystallization behavior of the recycled multilayer PET formulations. To facilitate the comparison of the effect of compatibilizer concentration, the thermograms were grouped according to compatibilizer family (EGMA, EMAGMA and EAA), allowing the concentration-dependent thermal response of each reactive system to be more clearly visualized.

The thermogram of the reference mPET exhibited two main endothermic transitions. A first melting peak was observed around 110–120 °C, which can be attributed to the melting of the polyethylene-rich phase present in the multilayer structure. The second and more intense endothermic peak appeared between 247 and 250 °C, corresponding to the melting temperature of PET. The presence of these two melting events confirms the multiphase nature of the recycled feedstock and indicates the coexistence of different polymer components within the system.

Comparison of the grouped thermograms revealed that the compatibilizers produced more noticeable changes in the polyethylene-rich melting region than in the PET melting peak. While the position of the PET melting peak remained essentially unchanged for all formulations, slight variations in the polyethylene melting region were observed depending on the compatibilizer type and concentration. This behavior suggests that the reactive compatibilizers predominantly influence the thermal organization of the polyethylene-rich phase rather than the crystalline structure of the PET-rich phase. After melt processing, the original multilayer architecture is disrupted, resulting in a heterogeneous morphology composed of a PET-rich continuous phase and a dispersed phase rich in polyethylene, as supported by the FESEM observations. Under these conditions, the compatibilizers are expected to localize preferentially at the interfaces between both phases, where they may modify the local molecular mobility and consequently influence the crystallization behavior of the polyethylene-rich dispersed phase.

It should also be noted that the glass transition of the PET-rich phase could not be clearly identified in the reference mPET because it overlaps with the onset of the polyethylene melting process. A similar behavior was observed for all EGMA-containing formulations, as well as for the EMAGMA-modified systems, where the overlapping thermal events prevented an accurate determination of the PET glass transition. In contrast, the PET glass transition became distinguishable in the EAA-containing formulations, with Tg values of 70.91 °C for mPET EAA_3 and 70.96 °C for mPET EAA_5. Although the origin of this behavior cannot be conclusively established, it suggests that EAA modifies the thermal organization of the heterogeneous recycled structure in a manner that allows the PET glass transition to be resolved more clearly.

The incorporation of EGMA, Figure 4, did not produce significant shifts in the position of either melting peak, indicating that the compatibilizer does not substantially modify the melting temperatures of the main polymeric constituents. However, subtle changes in the shape and intensity of the polyethylene-rich melting peak became progressively more evident with increasing EGMA content, particularly for the EGMA_5 formulation, whereas the PET melting peak remained practically unchanged.

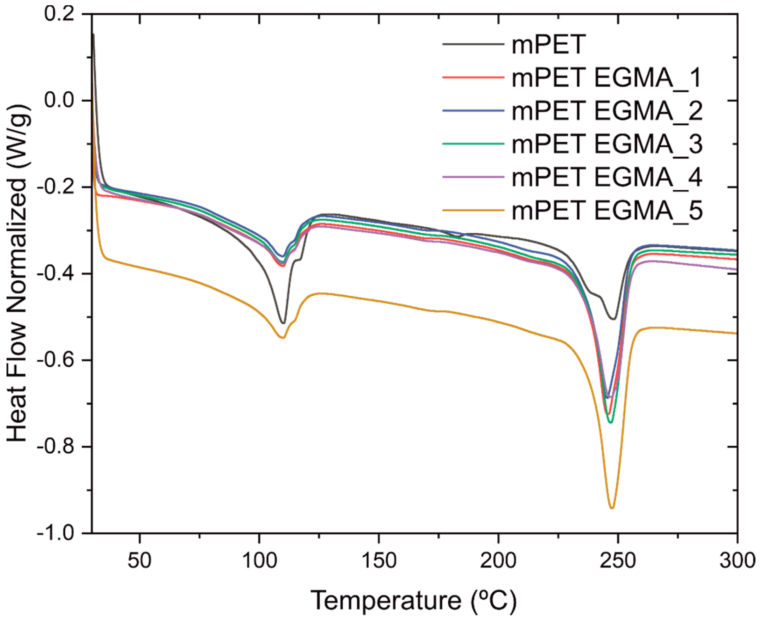


Figure 4. DSC thermograms of the recycled mPET and EGMA-modified formulations.

The reference mPET exhibited a PET melting enthalpy (ΔH_m) of 13.42 J/g, whereas all EGMA-modified formulations showed higher values, reaching a maximum of 21.28 J/g for the EGMA_5 formulation. Since the reported ΔH_m values were determined exclusively from the PET melting peak, the observed increase indicates that EGMA modifies the crystalline organization of the PET-rich phase. Although the exact PET content of the recycled multilayer material is unknown, and therefore the absolute degree of PET crystallinity cannot be calculated, the higher melting enthalpy suggests that a larger fraction of PET crystals contributes to the melting process after compatibilization.

The evolution of ΔH_m with EGMA concentration was not strictly linear, as intermediate formulations exhibited slight fluctuations. This behavior is expected for heterogeneous recycled multilayer systems, where the compatibilizer influences the interfacial interactions between the different polymer phases, which in turn may affect the crystallization behavior of the PET-rich phase during cooling. Overall, the results suggest that EGMA promotes modifications in the crystalline organization of PET without significantly altering its melting temperature.

Overall, the EGMA formulations preserve the characteristic melting transitions of both the polyethylene-rich and PET-rich phases while modifying the overall thermal response of the recycled multilayer system. The practically unchanged PET melting temperature indicates that the crystalline regions associated with the PET-rich phase remain largely unaffected within the investigated concentration range. In contrast, the more pronounced variations observed in the polyethylene-rich melting region suggest that EGMA mainly influences the thermal behavior of the dispersed polyethylene-rich phase after melt processing. This interpretation is consistent with the heterogeneous morphology observed by FESEM, where the original multilayer architecture evolves into a PET-rich continuous phase containing a dispersed polyethylene-rich phase.

The DSC thermograms of the EMAGMA-containing formulations are presented in Figure 5. Similarly to the EGMA-modified systems, the EMAGMA formulations exhibited two main endothermic transitions associated with the polyethylene-rich phase (approximately 115 °C) and the PET-rich phase (247–250 °C). No significant changes in the position of the melting peaks were observed after the incorporation of EMAGMA, indicating that the compatibilizer did not substantially modify the thermal transitions associated with the main polymeric components of the multilayer material.

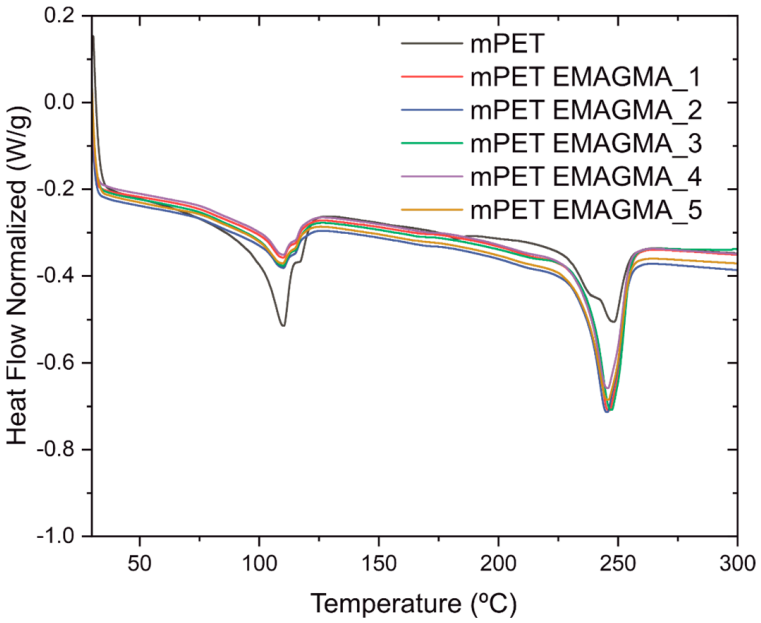


Figure 5. DSC thermograms of the recycled mPET and EMAGMA-modified formulations.

The incorporation of EMAGMA increased the PET melting enthalpy (ΔH_m) compared with the reference mPET. All EMAGMA-containing formulations exhibited higher ΔH_m values than the unmodified material, with the highest value corresponding to EMAGMA_5 (20.2 J/g). Since the reported ΔH_m values were determined exclusively from the PET melting peak, these results indicate that EMAGMA modifies the crystalline organization of the PET-rich phase. Although the exact PET content of the recycled multilayer material is unknown and the absolute degree of PET crystallinity cannot therefore be determined, the higher melting enthalpy suggests that a greater amount of crystalline PET contributes to the melting process after compatibilization.

Compared with the EGMA formulations, the EMAGMA thermograms exhibited a more homogeneous evolution as the compatibilizer concentration increased, with less pronounced fluctuations between intermediate formulations. This behavior suggests that EMAGMA produces a more gradual modification of the thermal organization of the

heterogeneous recycled structure while maintaining the characteristic melting transitions of both polymer phases.

The similarity between the thermal behavior of EGMA- and EMAGMA-containing formulations suggests that both glycidyl methacrylate-based compatibilizers influence the thermal response of the recycled material in a comparable manner. This similarity is consistent with the presence of glycidyl methacrylate functional groups in both compatibilizers, which are expected to promote comparable interfacial interactions within the heterogeneous polymer system. Furthermore, the absence of significant shifts in the PET melting temperature indicates that the compatibilization process did not adversely affect the thermal stability of the PET-rich phase.

As previously discussed for the EGMA systems, the more noticeable variations observed in the polyethylene-rich melting region compared with the PET melting peak suggest that EMAGMA predominantly influences the thermal organization of the polyethylene-rich dispersed phase. This observation is consistent with the heterogeneous morphology observed after melt processing, where the original multilayer architecture evolves into a PET-rich continuous phase containing a likely polyethylene-rich dispersed phase.

Overall, the DSC results indicate that EMAGMA modifies the thermal behavior of the recycled multilayer material while preserving the characteristic melting transitions of its constituent polymer phases. The thermal response observed for EMAGMA is therefore comparable to that obtained with EGMA, suggesting that both glycidyl methacrylate-based compatibilizers affect the recycled multilayer system through similar thermal mechanisms, despite the differences observed in their mechanical performance.

The DSC thermograms of the EAA-containing formulations are presented in Figure 6. Similarly to the EGMA- and EMAGMA-modified systems, two main endothermic transitions were observed, corresponding to the polyethylene-rich phase (approximately 115 °C) and the PET-rich phase (247–250 °C). The position of both melting peaks remained essentially unchanged after the incorporation of EAA, indicating that the compatibilizer does not significantly modify the melting temperatures of the main polymeric constituents present in the recycled multilayer material.

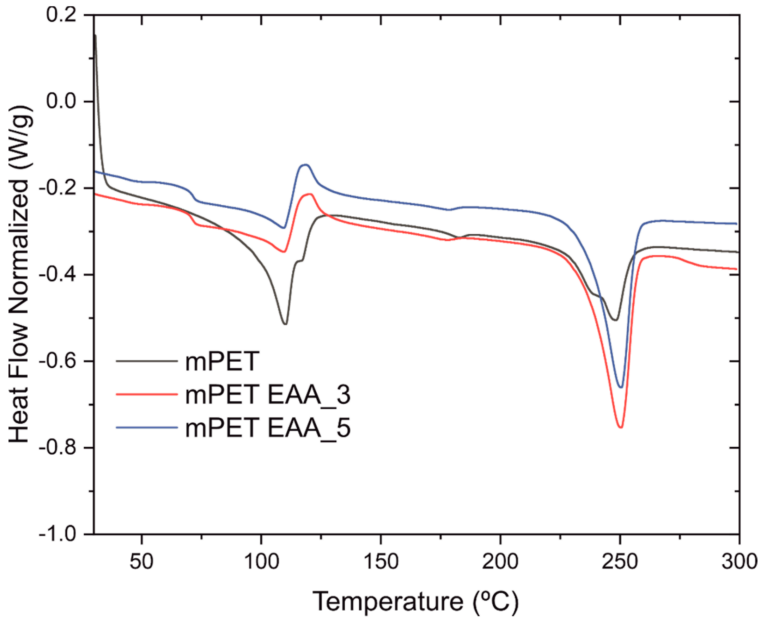


Figure 6. DSC thermograms of the recycled EAA-modified formulations.

The incorporation of EAA significantly increased the PET melting enthalpy (ΔH_m) of the recycled formulations. The reference mPET exhibited a ΔH_m value of 13.42 J/g,

whereas the EAA-containing formulations reached 33.60 J/g and 30.40 J/g for EAA_3 and EAA_5, respectively, corresponding to the highest values among all compatibilized systems investigated in this study. Since the reported ΔH_m values were determined exclusively from the PET melting peak, these results indicate that EAA produced the most pronounced modification of the crystalline organization of the PET-rich phase. Although the exact PET content of the recycled multilayer feedstock is unknown and the absolute degree of PET crystallinity cannot therefore be determined, the higher melting enthalpy suggests that a greater amount of crystalline PET contributes to the melting process after compatibilization.

Unlike the EGMA- and EMAGMA-containing formulations, the PET glass transition became distinguishable in the EAA systems, with T_g values of 70.91 °C for mPET EAA_3 and 70.96 °C for mPET EAA_5. Although the origin of this behavior cannot be conclusively established, it suggests that EAA modifies the thermal organization of the heterogeneous recycled structure in a different manner, allowing the PET glass transition to be resolved more clearly despite the overlap with the polyethylene melting process observed in the remaining formulations.

Interestingly, although the EAA-containing formulations exhibited the highest PET melting enthalpy (ΔH_m) values, they did not provide the greatest improvements in tensile ductility or impact resistance. This observation indicates that the thermal response of the compatibilized materials is not directly reflected in their mechanical performance. Instead, the superior mechanical behavior observed for the EGMA- and EMAGMA-based systems is more likely associated with more effective interfacial compatibilization between the polymer phases than with changes in the PET melting behavior alone. Therefore, an increase in PET melting enthalpy does not necessarily translate into superior mechanical performance, highlighting that the effectiveness of the compatibilization strategy is governed primarily by improved interfacial interactions rather than solely by modifications in the crystalline organization of the PET-rich phase.

Overall, the DSC results indicate that EAA produced the most pronounced modification of the thermal response of the recycled multilayer system than EGMA and EMAGMA while preserving the characteristic melting transitions associated with the constituent polymer phases. The appearance of a distinguishable PET glass transition further supports that EAA influences the heterogeneous polymer structure differently from the glycidyl methacrylate-based compatibilizers, although this different thermal behavior does not translate into superior mechanical performance.

Table 3 summarizes the PET melting enthalpy (ΔH_m) values obtained for all investigated formulations. All compatibilized systems exhibited higher PET melting enthalpy than the reference mPET, although the magnitude of the increase depended on the compatibilizer type and concentration. The highest ΔH_m values were obtained for the EAA-containing formulations, whereas the EGMA- and EMAGMA-based systems exhibited more moderate increases. Overall, these results indicate that the reactive compatibilizers influence the crystalline organization of the PET-rich phase to different extents. However, the observed thermal changes did not directly correlate with the mechanical performance of the materials, confirming that the superior tensile ductility and impact resistance achieved with EGMA and EMAGMA are primarily associated with more effective interfacial compatibilization rather than with changes in PET melting enthalpy alone.

2.3.2. Thermogravimetric Analysis (TGA)

The thermogravimetric parameters obtained from TGA analysis are summarized in Table 3 together with the melting enthalpy obtained by DSC, while the representative DTG curves are presented in Figure 7.

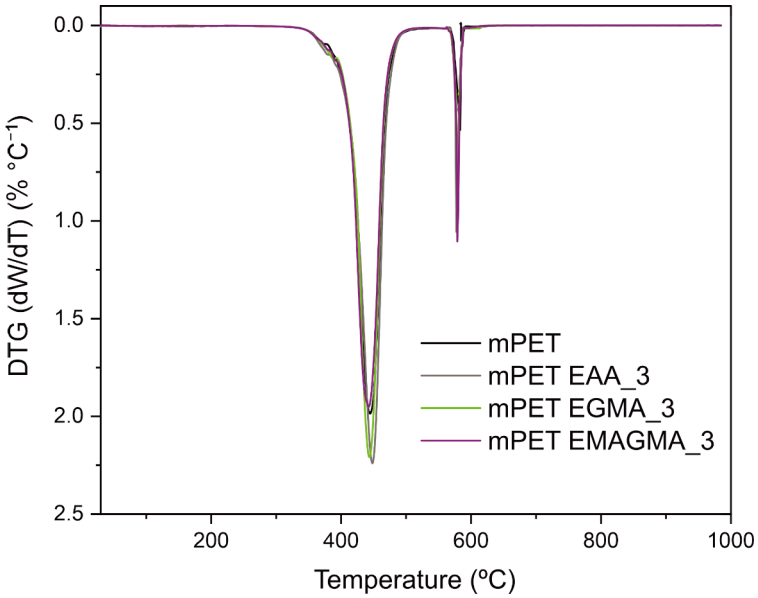


Figure 7. Representative DTG curves of the recycled mPET and selected compatibilized formulations.

The incorporation of different compatibilizers produced only minor variations in the thermal degradation behavior of the recycled multilayer formulations. The temperature corresponding to 5 wt.% mass loss ($T_{5\%}$) remained within a relatively narrow range (approximately 386–395 °C) for all investigated formulations, indicating that the addition of EAA, EGMA, or EMAGMA did not significantly affect the initial thermal stability of the recycled system.

Similarly, the onset degradation temperature (T_{onset}) showed only moderate variations among the formulations. Although slightly higher T_{onset} values were observed for some compatibilized formulations, particularly mPET EGMA_1 (439.11 ± 17 °C), no systematic trend with either compatibilizer type or concentration was identified. Moreover, the relatively large standard deviations suggest that these differences fell within the experimental variability of the measurements.

As shown in Figure 7, all formulations exhibited nearly identical DTG profiles, with the main degradation peak occurring within a narrow temperature interval. The similarity of the DTG curves indicates that the incorporation of EAA, EGMA and EMAGMA did not alter the degradation mechanism of the recycled multilayer material. A second sharp DTG peak was observed at higher temperatures, corresponding to the rapid oxidative combustion of the carbonaceous residue formed during pyrolysis following the programmed change of the purge atmosphere from nitrogen to oxygen. This feature is associated with the experimental procedure rather than with an additional degradation stage of the polymeric material.

The maximum degradation temperature (T_{max-1}) also remained relatively constant, ranging from approximately 437 to 448 °C. The EAA-modified formulations exhibited the highest T_{max-1} values, reaching 448.24 °C for mPET EAA_3. However, the differences among the formulations were small, indicating that the incorporation of the investigated compatibilizers did not substantially modify the thermal degradation behavior of the recycled multilayer material.

Overall, both the thermal parameters summarized in Table 3 and the DTG curves shown in Figure 7 demonstrate that the incorporation of EAA, EGMA, and EMAGMA preserves the thermal stability and degradation behavior of the recycled multilayer formulations.

2.4. FTIR Analysis

The FTIR spectrum of the recycled multilayer PET (mPET) (Figure 8) indicates the presence of a heterogeneous polymer system mainly composed of polyester and polyethylene-based components, confirming the complex multilayer nature of the recycled material. The main absorption bands identified in the spectrum are summarized in Table 4.

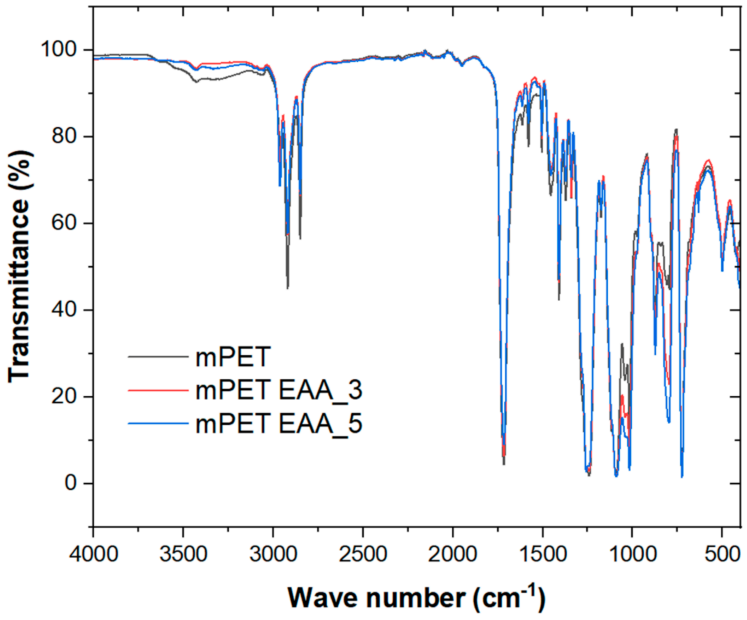


Figure 8. FTIR spectra of the mPET and EAA formulations.

Table 4. Assignment of the main absorption bands identified in the FTIR spectra of recycled mPET.

Peak (cm^{-1})	Functional Group Assignment	Corresponding Polymer
724	CH_2 rocking vibration	PE
800	Aromatic ring vibrations	PET
873	Aromatic C–H out-of-plane bending (crystalline PET)	Crystalline PET domains
1018	C–O stretching	PET
1092	C–O stretching	PET
1407	CH_2 bending vibration	PE, PET
1716	C=O stretching of ester groups	PET
2850	CH_2 asymmetric stretching	PE
2919	CH_2 asymmetric stretching	PE
2958	CH stretching vibration	PE

The absorption band located at 724 cm^{-1} is assigned to the CH_2 rocking vibration characteristic of polyethylene, confirming the presence of a polyethylene-rich phase within the recycled multilayer structure. The absorption bands observed at 800, 873, 1018, 1092, and 1716 cm^{-1} are characteristic of PET structures. These signals are associated with typical vibrational modes of polyester materials, including C–O stretching, C=O stretching of ester groups, and aromatic ring vibrations. In particular, the band at 873 cm^{-1} has been associated with the crystalline phase of PET, suggesting the presence of ordered regions within the polyester phase. In addition, the peaks located at 1407, 2850, 2919, and 2958 cm^{-1} are attributed to CH_2 and CH_3 stretching and deformation vibrations characteristic of polyethylene-based materials. These signals confirm the presence of polyolefin components within the multilayer structure (Table 4).

Overall, the FTIR results confirm that the recycled feedstock contains both polyester and polyolefin phases, which is consistent with its origin as a multilayer packaging material. These findings are in agreement with the DSC results, where distinct thermal transitions associated with PET-rich and polyethylene-rich phases were identified.

Regarding the effect of the compatibilizers (EAA, EGMA, and EMAGMA) on the FTIR spectra, the spectra were grouped according to compatibilizer family to facilitate comparison among the different compatibilizer concentrations (Figures 8–10). Overall, all compatibilized formulations exhibited FTIR spectra very similar to that of the reference mPET. No new absorption bands or significant peak shifts were observed after the incorporation of the reactive compatibilizers, irrespective of compatibilizer type or concentration.

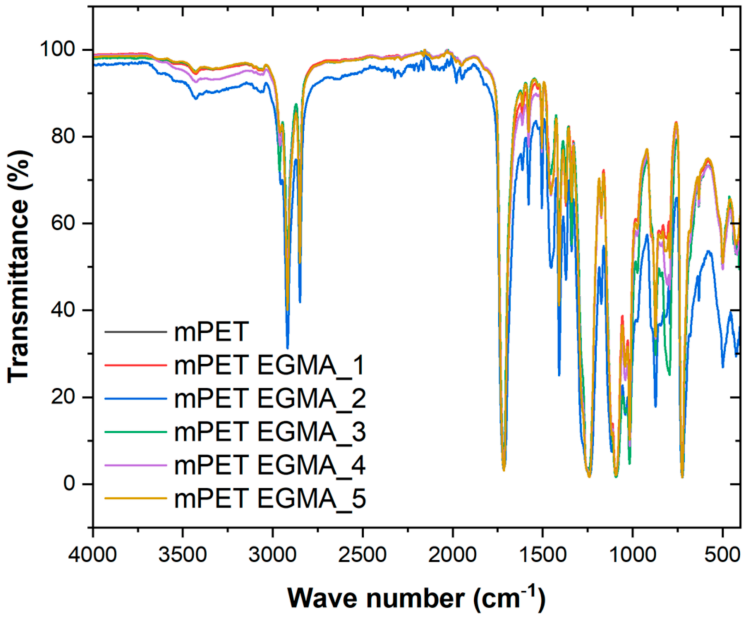


Figure 9. FTIR spectra of the mPET and EGMA formulations.

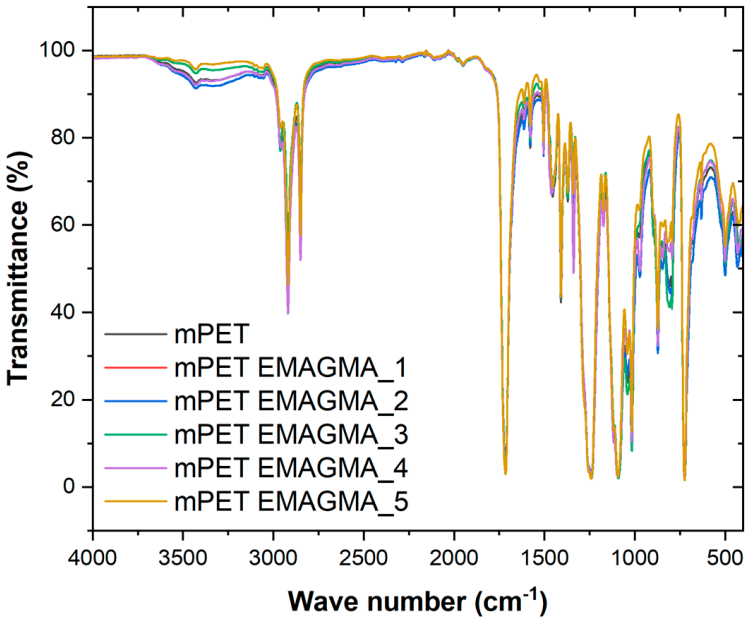


Figure 10. FTIR spectra of the mPET and EMAGMA formulations.

The main differences observed among the spectra were limited to slight variations in band intensity, particularly within the fingerprint region (approximately 1200–900 cm^{-1}),

where the characteristic C–O stretching vibrations of PET are located, and to a lesser extent within the C–H stretching region between 2850 and 2960 cm^{-1}. However, these variations were relatively small and no systematic trend with increasing compatibilizer concentration could be established.

The absence of new absorption bands does not necessarily exclude the occurrence of reactive compatibilization during melt processing. EAA contains carboxylic acid groups, whereas EGMA and EMAGMA contain glycidyl methacrylate functionalities, which are capable of reacting with terminal hydroxyl and carboxyl groups present in PET chains. Nevertheless, because the compatibilizers were incorporated at relatively low concentrations (1–5 wt.%) and the recycled feedstock consisted of a complex heterogeneous PET/PE multilayer system, any newly formed chemical bonds were expected to be present at concentrations below the detection limit of ATR-FTIR. Consequently, the characteristic absorption bands of the PET-rich phase remained dominant and masked any subtle chemical modifications occurring at the polymer interfaces.

These observations are in agreement with previous studies on multilayer PET packaging waste, where FTIR analyses confirmed the coexistence of polyester and polyolefin phases within complex multilayer structures [3,9]. Van Vliet et al. also reported characteristic PET ester bands together with polyolefin CH stretching vibrations in PET-PE multilayer trays, confirming the heterogeneous composition of these waste streams [9].

Although ATR-FTIR did not reveal substantial chemical modifications after compatibilization, the mechanical characterization demonstrated significant improvements in tensile and impact properties, particularly for the EGMA- and EMAGMA-based formulations. Therefore, the improvements in mechanical performance are more likely associated with interfacial interactions and morphological refinement promoted during reactive melt processing than with extensive chemical modifications detectable by ATR-FTIR.

Overall, the FTIR results indicate that the reactive compatibilizers preserve the characteristic chemical structure of the recycled multilayer material while promoting modifications that are primarily expressed through changes in interfacial interactions and phase morphology rather than through the appearance of new infrared absorption bands.

2.5. Contact Angle Measurements

Table 5 summarizes the contact angle values measured for the reference mPET and the formulations modified with EAA, EGMA, and EMAGMA. These measurements provide information on the effect of the compatibilizers on the surface wettability of the recycled multilayer system.

The data indicated a slight increase in the contact angle as the EAA content increased. The base material, mPET, exhibited the lowest contact angle (70.67°), while mPET EAA_5 had the highest (73.3°). This suggests that the addition of EAA slightly affects the surface properties, potentially resulting in a moderate reduction in surface wettability. However, the changes were relatively small, indicating that the modification does not drastically alter the wettability of the surface.

The contact angle values suggest that the addition of EGMA influences the surface properties of mPET. The highest contact angle was observed for mPET EGMA_2 (78.67°), indicating a more hydrophobic surface. However, for higher EGMA content (EGMA_3, EGMA_4, EGMA_5), the contact angle decreased slightly, suggesting that the influence of EGMA on surface wettability does not follow a linear trend with compatibilizer concentration. Compared to unmodified mPET (70.67°), all modified samples showed higher in contact angle values, indicating a general decrease in surface wettability after compatibilization.

Table 5. Water contact angle values of the recycled mPET formulations modified with EAA, EGMA, and EMAGMA.

Sample	Contact Angle (°)
mPET	70.7 ± 3.5
mPET EAA_3	72.0 ± 3.6
mPET EAA_5	73.3 ± 3.5
mPET EGMA_1	74.6 ± 2.5
mPET EGMA_2	78.7 ± 2.3
mPET EGMA_3	73.3 ± 3.7
mPET EGMA_4	74.3 ± 4.5
mPET EGMA_5	74.0 ± 2.6
mPET EMAGMA_1	71.7 ± 5.1
mPET EMAGMA_2	74.3 ± 3.2
mPET EMAGMA_3	69.0 ± 3.6
mPET EMAGMA_4	77.7 ± 3.5
mPET EMAGMA_5	69.6 ± 4.0

The contact angle results indicate that the modification with EMAGMA did not follow a clear increasing or decreasing trend. mPET EMAGMA_4 exhibited the highest contact angle (77.7°), suggesting a reduction in wettability compared to unmodified mPET (70.67°). However, mPET EMAGMA_3 and mPET EMAGMA_5 showed lower values (69.0° and 69.6°, respectively), indicating that in some cases, the modification may slightly enhance wettability rather than reducing it. This variability suggests that the effect of EMAGMA on the surface properties may depend on specific interactions between the polymer matrix and the modifying agent rather than following a simple concentration-dependent trend. Furthermore, the relatively large standard deviations observed for some formulations indicate a certain variability in surface behavior, which may be related to the heterogeneous nature of the recycled multilayer material.

Overall, the contact angle measurements indicate that the incorporation of EAA, EGMA, and EMAGMA only moderately affects the surface wettability of recycled mPET. Among the evaluated compatibilizers, EGMA generally produced the highest contact angle values, whereas EAA and EMAGMA exhibited more limited and less consistent effects.

2.6. Density Measurements

Table 6 summarizes the density values obtained for the reference mPET and the compatibilized formulations. Overall, only minor variations in density were observed after the incorporation of EAA, EGMA, and EMAGMA, with all formulations exhibiting values between 1.22 and 1.25 g/cm^3. Considering the low compatibilizer contents investigated (1–5 phr), these limited changes were expected and indicate that the compatibilizers do not substantially modify the overall composition or mass-to-volume relationship of the recycled multilayer material. Furthermore, the absence of significant density variations suggests that the processing conditions did not introduce appreciable internal porosity. Despite the nearly constant density, notable differences in tensile and impact properties were observed, indicating that the improved mechanical performance arises primarily from enhanced interfacial compatibilization rather than from changes in the bulk density of the material.

Table 6. Density values of the recycled mPET formulations modified with EAA, EGMA, and EMAGMA.

Sample	Density (g/cm^3)
mPET	1.23 ± 0.10
mPET EAA_3	1.24 ± 0.09
mPET EAA_5	1.22 ± 0.12
mPET EGMA_1	1.24 ± 0.10
mPET EGMA_2	1.24 ± 0.09
mPET EGMA_3	1.24 ± 0.10
mPET EGMA_4	1.24 ± 0.10
mPET EGMA_5	1.22 ± 0.12
mPET EMAGMA_1	1.24 ± 0.09
mPET EMAGMA_2	1.25 ± 0.07
mPET EMAGMA_3	1.24 ± 0.10
mPET EMAGMA_4	1.24 ± 0.09
mPET EMAGMA_5	1.23 ± 0.14

2.7. Morphological Characterization

Figure 11 presents representative FESEM micrographs of the reference mPET fracture surface acquired at magnifications of 500× and 1000×. The fracture surface exhibited a heterogeneous morphology characterized by dispersed domains with a broad size distribution embedded within a continuous matrix, confirming the multiphase nature of the recycled multilayer material. Similar heterogeneous morphologies have been reported for mechanically recycled multilayer packaging wastes and uncompatibilized PET/polyethylene blends, where the immiscibility between the constituent polymers leads to coarse dispersed domains and poor interfacial adhesion between phases [10,12].

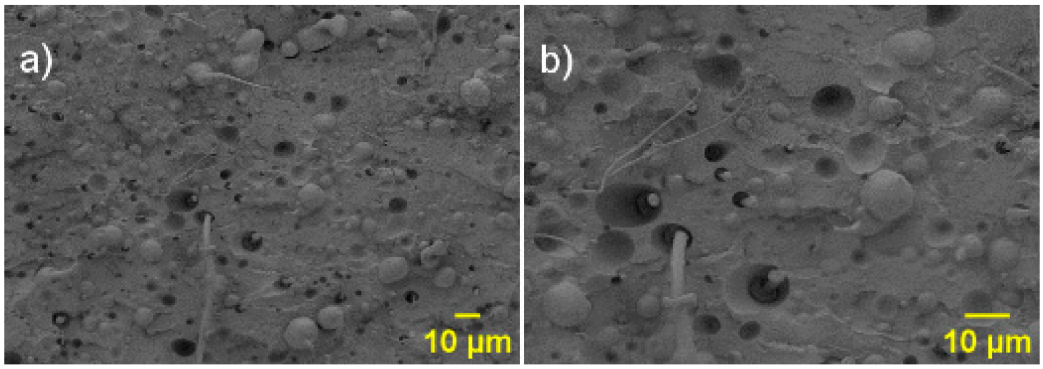


Figure 11. FESEM micrographs of the reference mPET fracture surface at (**a**) 500× and (**b**) 1000×.

At higher magnification (1000×), embedded dispersed domains together with numerous pull-out cavities were clearly distinguished. The presence of these cavities indicates that part of the dispersed domains detached from the surrounding matrix during impact fracture, reflecting limited interfacial adhesion between the polymeric phases. Similar fracture features, including particle debonding and heterogeneous dispersed morphologies, have been reported for recycled multilayer systems and PET/polyethylene blends before compatibilization [10,12].

To complement the qualitative observations, the morphology was quantitatively analyzed by measuring the equivalent circular diameter (ECD) of the embedded dispersed domains from representative FESEM micrographs. The reference mPET exhibited an average ECD of 3.70 ± 2.17 µm, together with a broad domain size distribution, confirming the coarse and heterogeneous morphology of the dispersed phase. This behavior is charac-

teristic of immiscible polymer systems in which insufficient interfacial interactions hinder efficient stress transfer across the interface [12,13,21]. The quantitative analysis therefore provides the baseline morphology against which the effectiveness of the different reactive compatibilizers can be assessed.

Figure 12 presents representative FESEM micrographs of the mPET formulations containing 3 and 5 phr of EAA. Both formulations exhibited a heterogeneous fracture morphology characterized by dispersed domains with different sizes embedded within the continuous matrix, together with numerous pull-out cavities generated during impact fracture. These features indicate that the addition of EAA does not substantially modify the multiphase morphology of the recycled multilayer material, suggesting that interfacial adhesion between the polymeric phases remains limited.

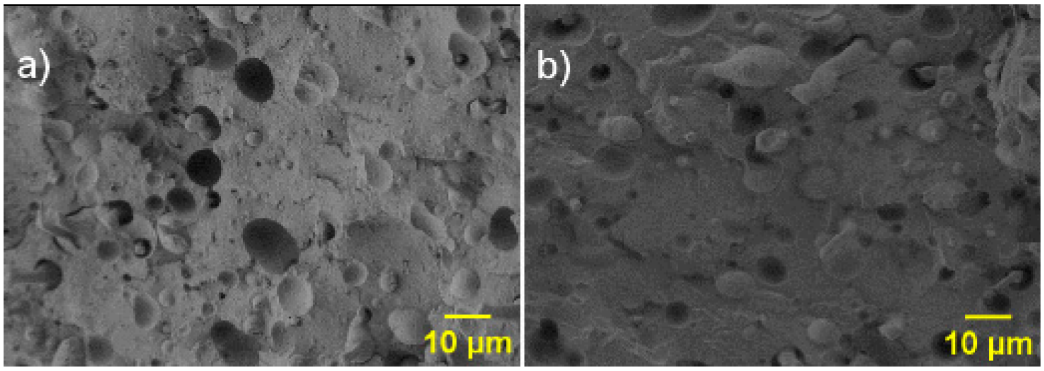


Figure 12. FESEM micrographs of the fracture surfaces of the mPET formulations modified with (**a**) 3 phr and (**b**) 5 phr EAA.

Quantitative image analysis supports these observations. The average equivalent circular diameter (ECD) of the dispersed domains in the mPET EAA_3 formulation was 4.02 ± 2.30 µm, which was not significantly different from that of the reference mPET according to one-way ANOVA followed by Tukey's multiple comparison test ($p > 0.05$). Likewise, the broad domain size distribution remained comparable to that of the uncompatibilized material, indicating that EAA produced only a limited refinement of the dispersed morphology.

These observations are consistent with the mechanical results, where EAA produced only modest improvements in tensile ductility and impact resistance. Although EAA has been reported to improve the interfacial adhesion of PET/polyethylene blends when an adequate density of reactive acrylic acid groups is available [13], its effectiveness strongly depends on the blend composition and the interfacial reaction efficiency. Similar heterogeneous morphologies have also been reported for mechanically recycled multilayer materials in which limited compatibilization results in coarse dispersed domains and incomplete interfacial adhesion [10,11].

Figure 13 presents representative FESEM micrographs of the mPET formulations containing 2, 3, 4, and 5 phr of EGMA. All EGMA-containing formulations exhibited a more homogeneous fracture morphology than the reference mPET, characterized by a finer dispersion of the dispersed domains within the continuous matrix and a lower occurrence of large pull-out cavities. Among them, the EGMA_3 formulation displayed the most uniform microstructure, with smaller dispersed domains and a more homogeneous spatial distribution throughout the fracture surface, suggesting improved interfacial adhesion between the polymeric phases.

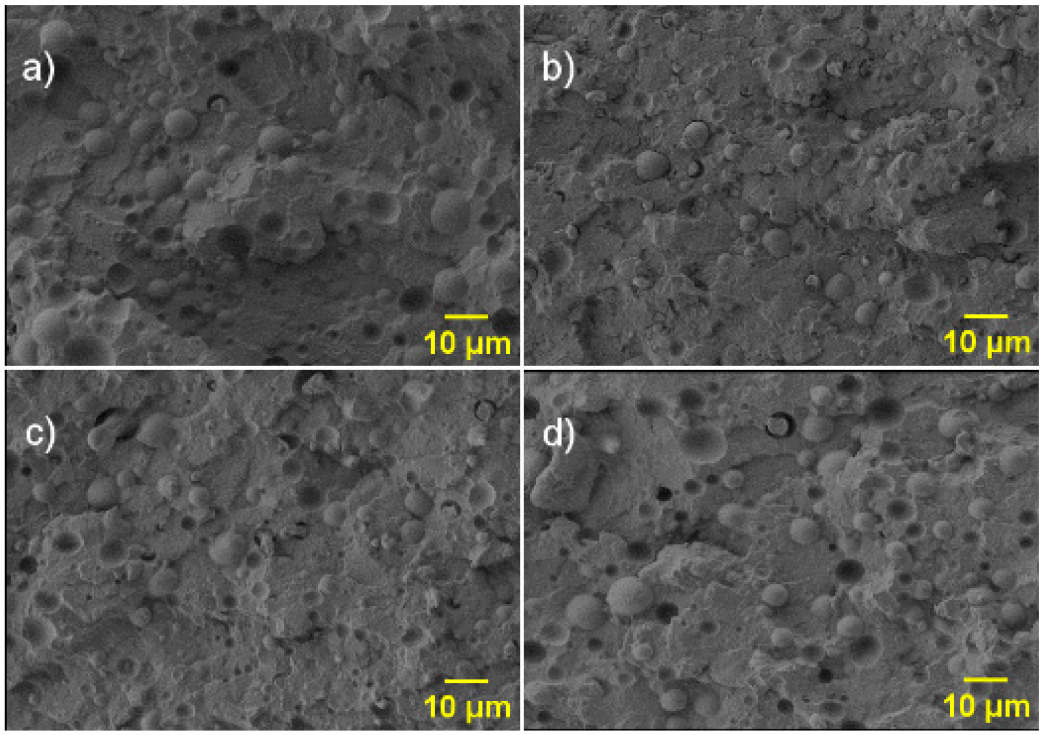


Figure 13. FESEM micrographs of the mPET formulations modified with EGMA at (**a**) 2 phr, (**b**) 3 phr, (**c**) 4 phr, and (**d**) 5 phr.

The qualitative observations are supported by the quantitative image analysis. The EGMA_3 formulation exhibited an average equivalent circular diameter (ECD) of 2.74 ± 1.26 µm, representing the smallest dispersed-domain size among the analyzed formulations. One-way ANOVA followed by Tukey's multiple comparison test confirmed a statistically significant reduction in ECD with respect to the reference mPET ($p < 0.05$), demonstrating the effectiveness of EGMA in refining the dispersed morphology. Furthermore, the lower standard deviation indicates a narrower domain size distribution, reflecting a more homogeneous dispersion of the dispersed phase.

The observed morphological refinement is consistent with the proposed compatibilization mechanism of glycidyl methacrylate-functionalized copolymers. The epoxy groups of EGMA can react with terminal hydroxyl and carboxyl groups present in polyester-rich phases, while the polyethylene backbone remains compatible with the polyolefin-rich phase, reducing the interfacial tension and promoting stronger interfacial interactions [12,13]. Previous studies on immiscible PET/polyethylene blends have demonstrated that the morphology of these systems is primarily governed by the size, size distribution, and shape of the dispersed phase, with finer and more homogeneous morphologies leading to improved interfacial interactions and enhanced mechanical performance [13,20].

Similar reductions in dispersed-domain size and improvements in phase homogeneity have been reported for compatibilized PET/polyethylene blends and recycled multilayer polymer systems [10,12,13,22]. The improved morphology is also consistent with the mechanical performance of EGMA_3, which exhibited the best balance between tensile strength and elongation at break among the investigated formulations.

Figure 14 presents representative FESEM micrographs of the mPET formulations containing 2, 3, 4, and 5 phr of EMAGMA. Compared with the reference mPET, all EMAGMA-modified formulations exhibited a more homogeneous fracture morphology, characterized by a finer and more uniform dispersion of the dispersed domains within the continuous matrix. In addition, the number of large pull-out cavities was reduced, while the dispersed domains appeared better integrated into the surrounding matrix. Qualitatively,

the formulations containing 4 and 5 phr of EMAGMA exhibited slightly more continuous fracture surfaces, although the overall morphological differences among the EMAGMA formulations were relatively small.

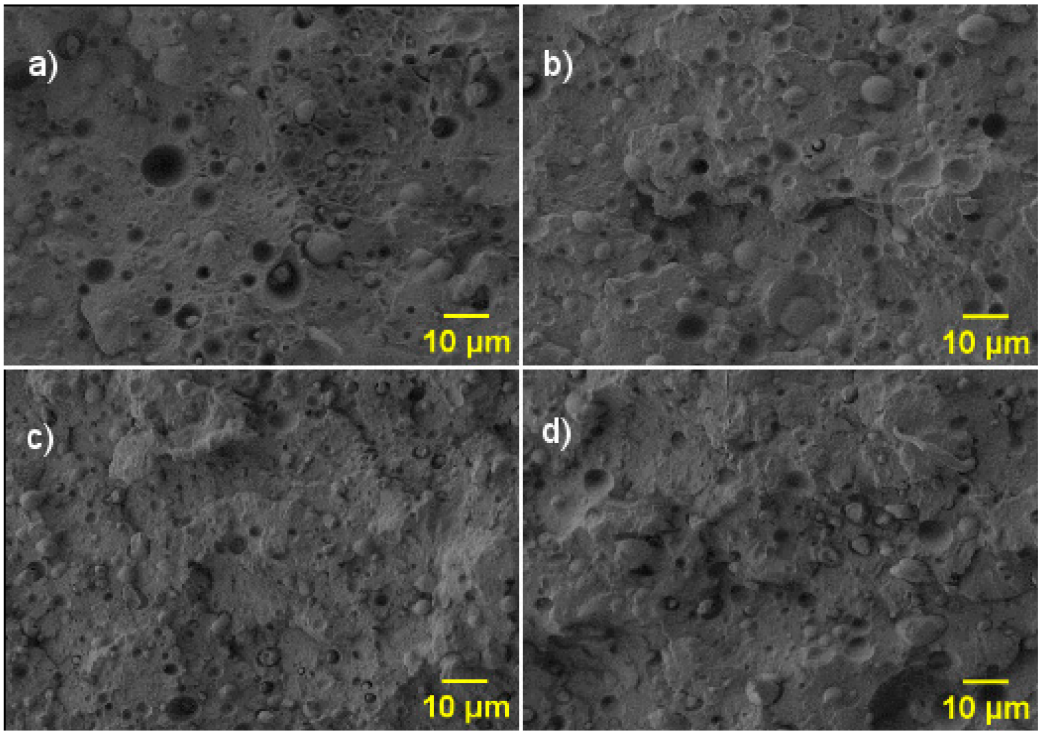


Figure 14. FESEM micrographs of the mPET formulations modified with EMAGMA at (**a**) 2 phr, (**b**) 3 phr, (**c**) 4 phr, and (**d**) 5 phr.

The quantitative image analysis supports these observations. The EMAGMA_3 formulation exhibited an average equivalent circular diameter (ECD) of 3.15 ± 1.49 µm (Figure 15), corresponding to an intermediate dispersed-domain size between the reference mPET and the EGMA_3 formulation. Although the reduction in ECD was not statistically significant with respect to the reference material ($p > 0.05$), the narrower domain size distribution together with the qualitative FESEM observations indicates a tendency toward a more homogeneous dispersion of the dispersed phase.

The observed morphological refinement is consistent with the expected compatibilization effect of EMAGMA. The glycidyl methacrylate and maleic anhydride functionalities are expected to promote interfacial interactions with the polyester-rich phase, while the polyethylene backbone remains compatible with the polyolefin-rich phase, thereby reducing interfacial tension and favoring a finer dispersion of the dispersed domains [12,13,20]. These observations are also in agreement with the mechanical results, as the EMAGMA-modified formulations exhibited higher elongation at break and impact strength than the reference material, indicating that the more homogeneous morphology contributed to a more efficient stress transfer across the polymer interfaces [10,12,13,22,23].

To provide a quantitative comparison of the morphological changes induced by the different reactive compatibilizers, the equivalent circular diameter (ECD) of the dispersed domains was measured from representative FESEM micrographs (1000×). As shown in Figure 15, the reference mPET and the EAA-modified formulation exhibited the largest dispersed-domain sizes and broadest distributions, whereas EGMA_3 produced the smallest average ECD and the narrowest size distribution. The EMAGMA_3 formulation showed an intermediate behavior, with a tendency toward finer and more homogeneous dispersed

domains than the reference material. These results are in good agreement with the qualitative FESEM observations and support the superior compatibilization efficiency of EGMA.

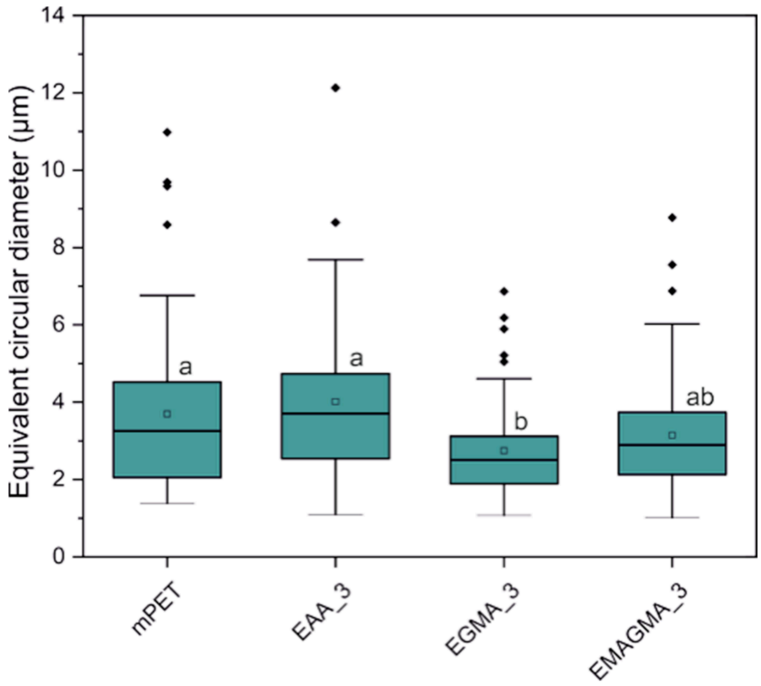


Figure 15. Distribution of the equivalent circular diameter (ECD) of dispersed domains measured from representative FESEM micrographs (1000×) of the reference mPET and selected compatibilized formulations. The box represents the interquartile range (25–75%), the horizontal line indicates the median, whiskers correspond to 1.5 × IQR, and symbols (◆) represent outliers. Different letters indicate statistically significant differences according to one-way ANOVA followed by Tukey's multiple comparison test ($p < 0.05$).

The quantitative and qualitative morphological analyses consistently demonstrate the beneficial effect of reactive compatibilization on the recycled multilayer material. Among the investigated compatibilizers, EGMA produced the greatest refinement of the dispersed morphology, exhibiting the smallest average equivalent circular diameter (ECD) and the only statistically significant reduction in dispersed-domain size compared with the reference mPET. EMAGMA also promoted a more homogeneous phase distribution and a tendency toward smaller dispersed domains, although these changes were not statistically significant. These observations are consistent with previous studies reporting that reactive compatibilizers reduce interfacial tension, improve phase dispersion, and promote finer dispersed morphologies in recycled multilayer systems and PET/polyethylene blends [11–13]. These findings are in excellent agreement with the work of Ronkay, who demonstrated that the mechanical performance of immiscible PET/HDPE blends is strongly governed by the size, distribution, and morphology of the dispersed phase [20]. Likewise, several authors have reported that reactive compatibilizers reduce phase separation, promote finer dispersed morphologies, and improve interfacial stress transfer in PET/polyolefin systems [10,12,13,22,23].

Overall, the morphological refinement observed in the present study is in good agreement with the tensile and impact results, confirming that improved phase dispersion and interfacial compatibility are the primary factors governing the enhanced mechanical behavior of the compatibilized recycled multilayer PET formulations.

3. Discussion

The results obtained in this study demonstrate that the performance of recycled multilayer PET (mPET) waste can be significantly improved through reactive compatibilization, although the effectiveness strongly depends on the chemical nature of the compatibilizer. Among the systems investigated, glycidyl methacrylate-based compatibilizers (EGMA and EMAGMA) consistently outperformed ethylene-acrylic acid (EAA), both in terms of mechanical performance and morphological development, highlighting the importance of compatibilizer functionality in heterogeneous recycled polymer systems.

It should be noted that the recycled material investigated in this study corresponds to shredded post-industrial multilayer packaging waste (production scraps and defective materials) supplied by an industrial partner. Consequently, the exact composition of the individual polymer layers and the molecular weight of each component were not available. The objective of this work was not to investigate the reaction mechanisms associated with a model polymer blend of known composition, but rather to comparatively evaluate the effectiveness of different commercial compatibilizers under identical processing conditions using the same batch of industrial recycled feedstock. Therefore, the differences observed among the formulations reflect the relative performance of the investigated compatibilizers under equivalent experimental conditions. Future studies including detailed compositional and molecular weight characterization would contribute to a better understanding of the compatibilization mechanisms involved in complex multilayer recycled systems.

3.1. Reactive Compatibilization Mechanisms in Polyester/Polyolefin Blends

Poly(ethylene terephthalate) (PET) and polyethylene (PE) are intrinsically immiscible because of their different chemical structures and polarities, resulting in poor interfacial adhesion, coarse phase morphology and limited stress transfer between both phases. Consequently, reactive compatibilization has become one of the main strategies for improving the performance of recycled PET/polyolefin blends, particularly those obtained from post-consumer or post-industrial multilayer packaging waste. Effective compatibilizers generally combine reactive or polar functional groups capable of interacting with PET with an olefinic backbone that exhibits affinity for the polyethylene-rich phase. Their localization at the interface promotes improved interfacial adhesion, finer phase dispersion, and more efficient stress transfer throughout the material.

Among the compatibilizers investigated in the present work, EGMA and EMAGMA contain glycidyl methacrylate (GMA) units bearing epoxy groups. These epoxy functionalities may react with the hydroxyl and carboxyl end groups of PET during melt processing, generating grafted structures that remain preferentially located at the PET/polyolefin interface owing to the ethylene backbone of the compatibilizer. The importance of compatibilizer localization during melt blending was already demonstrated by Dagli and Kamar, who showed that the addition sequence significantly influenced the morphology and mechanical properties of HDPE/PET blends [12]. More recently, Tang et al. confirmed that epoxy-functionalized ethylene copolymers exhibit a preferential interfacial location and provide stronger interactions with PET than other commercial compatibilizers, highlighting that compatibilization efficiency depends not only on the reactive group, but also on the molecular architecture of the compatibilizer [21].

A different mechanism has been proposed for acrylic acid-functionalized copolymers such as EAA. In these materials, the polyethylene backbone maintains compatibility with the polyolefin phase, whereas the acrylic acid groups can establish hydrogen bonding and other polar interactions with PET. Kim et al. demonstrated that the incorporation of poly(ethylene-co-acrylic acid) into PET/HDPE blends reduced the dispersed-phase dimensions and improved impact performance, particularly when HDPE constituted the contin-

uous phase. Nevertheless, the authors suggested that these improvements were mainly associated with enhanced interfacial adhesion rather than extensive covalent coupling, indicating that secondary interactions may play a significant role in the compatibilization process [13].

Maleic anhydride-containing compatibilizers have also been widely investigated for the recycling of heterogeneous polymer mixtures. Polymeric maleated compatibilizers combine an olefinic backbone with reactive anhydride groups that may interact with polar species present in polyester-rich phases, while simultaneously remaining compatible with the polyolefin matrix. However, their effectiveness depends strongly on the molecular architecture of the compatibilizer and on its ability to remain localized at the interface during melt processing. In contrast, free maleic anhydride lacks a polymeric backbone and therefore its contribution relies exclusively on reactions occurring during processing, without the inherent ability to stabilize the interface.

The relevance of these compatibilization mechanisms becomes particularly evident in the recycling of multilayer flexible packaging, where PET, PE, and additional barrier layers coexist within the same waste stream. Moreno and Saron demonstrated that the incorporation of compatibilizers significantly improved the mechanical behavior of recycled LDPE/polyamide multilayer waste by enhancing interfacial interactions between otherwise incompatible polymers [10]. Similarly, Uehara et al. showed that compatibilization constitutes one of the key parameters controlling the successful mechanical recycling of multilayer flexible packaging, highlighting the importance of processing conditions together with compatibilizer selection [15]. More recently, Turriziani et al. reported that maleic anhydride can also improve the mechanical recycling of multilayer flexible packaging, although its effectiveness depends on the formulation and processing conditions, suggesting that the reactive functionality alone does not guarantee efficient compatibilization [11]. These studies collectively highlight that the effectiveness of reactive compatibilization is governed by the combined influence of chemical functionality, molecular architecture, interfacial localization, and processing history rather than by the reactive group itself.

Accordingly, the behavior of EAA, EGMA, EMAGMA, EMA, and MA investigated in the present work is interpreted considering both their chemical functionality and molecular architecture, together with their potential ability to localize at the interfaces present in the recycled multilayer system. Therefore, the differences observed in the mechanical, thermal, and morphological properties are discussed not only in terms of the reactive groups present in each compatibilizer, but also considering the complex morphology of the recycled multilayer feedstock.

3.2. Effect of Compatibilizers on Material Properties

The mechanical behavior clearly shows that tensile strength alone is not a sufficient indicator of compatibilization efficiency, as more relevant differences were observed in elongation at break and impact resistance. In particular, EMAGMA exhibited an exceptional increase in ductility, reaching values close to 194%, which represents a substantial enhancement compared to the reference mPET. This behavior suggests that EMAGMA may contribute to a more effective stress distribution within the heterogeneous multilayer structure during deformation. The simultaneous maintenance of tensile strength close to that of the reference material further indicates that this compatibilizer achieves a favorable balance between stiffness retention and toughness enhancement, which is often difficult to obtain in recycled polymer blends.

EGMA also demonstrated a clear improvement in ductility and impact resistance, although its effect was slightly less pronounced than EMAGMA. This difference may be related to the additional comonomer present in EMAGMA, which could increase chain

mobility and favor interactions with the different phases present in the recycled multilayer feedstock. As a result, EMAGMA appears to form a more efficient compatibilized interphase, which translates into improved energy absorption during both tensile and impact loading.

In contrast, EAA showed limited compatibilization efficiency. Although low concentrations resulted in a moderate increase in elongation at break, higher loadings led to a deterioration in mechanical performance, particularly in terms of ductility. This suggests that EAA does not provide the same level of toughening efficiency as EGMA and EMAGMA in this system. The reduction in tensile strength observed at higher concentrations further supports this hypothesis, indicating that excessive softening of the matrix may weaken the structural integrity of the recycled material without significantly improving phase adhesion.

The morphological observations obtained by FESEM support the mechanical results. The reference mPET exhibited a typical heterogeneous structure with dispersed domains, voids, and interfacial defects, which act as stress concentration points during deformation. After compatibilization, particularly with EGMA and EMAGMA, a more homogeneous morphology was observed, characterized by a more uniform distribution of dispersed domains and fewer large cavities. This reduction in phase separation is directly correlated with the improved mechanical performance, confirming that interfacial adhesion is the key mechanism governing property enhancement in these systems.

Among all formulations, the EMAGMA-modified samples showed the most refined morphology, with a noticeable reduction in cavity formation and better integration of dispersed phases within the matrix. This morphological improvement explains the exceptionally high elongation at break and impact strength values observed experimentally. The results suggest that EMAGMA improved phase dispersion and promoted stronger interfacial interactions, which reduce crack propagation and delay catastrophic failure under mechanical loading.

The impact strength results further reinforce these conclusions. The dramatic increase observed for EMAGMA-containing formulations, particularly at higher loadings, indicates a significant improvement in energy dissipation mechanisms. This enhancement is likely associated with the ability of the compatibilized interphase to absorb and redistribute stress more efficiently, preventing the rapid propagation of microcracks. EGMA follows the same trend but with lower efficiency, while EAA does not significantly contribute to impact resistance improvement, confirming its limited compatibilization capability.

Thermal analysis by DSC indicates that all compatibilizers influence the thermal response of the recycled system by increasing the apparent enthalpy of melting (ΔH_m). However, these changes do not correlate directly with mechanical performance. In particular, EAA showed the highest ΔH_m values but the poorest mechanical improvements, suggesting that thermal response alone cannot explain the observed mechanical behavior. Because the exact PET/PE/EVOH composition of the multilayer feedstock is unknown, these changes cannot be directly attributed to variations in the crystallinity of a specific polymer phase. The absence of significant shifts in melting temperatures indicates that the main melting transitions of the recycled multilayer material remain largely preserved after compatibilization.

Interestingly, although the compatibilizers modified the melting enthalpy measured by DSC, these changes were not accompanied by significant variations in the degradation temperatures obtained by TGA. This indicates that the compatibilizers mainly affect the organization and morphology of the heterogeneous recycled system without substantially modifying its intrinsic thermal degradation resistance. The preservation of the thermal stability after compatibilization is particularly relevant for industrial recycling processes,

as it indicates that the incorporation of EGMA and EMAGMA does not compromise the processing window of the recycled multilayer material. This is especially important for extrusion and injection molding operations, where thermal degradation during repeated processing cycles can severely limit the reuse of recycled polymers. Similarly, FTIR analysis confirmed that no new absorption bands or significant spectral shifts were detectable within the resolution of the technique. This indicates that the compatibilization mechanisms are not associated with extensive bulk chemical modification detectable by FTIR-ATR. Instead, the improvements observed in mechanical performance are more likely related to localized interfacial interactions and morphological changes, as supported by FESEM observations.

Taken together, the DSC, TGA, FTIR, and FESEM results indicate that the enhanced mechanical performance of the EGMA- and EMAGMA-containing formulations is primarily associated with morphological modifications rather than significant changes in the chemical structure or intrinsic thermal stability of the recycled multilayer material.

Surface wettability and density measurements further support the conclusion that compatibilization primarily affects interfacial rather than bulk properties. The relatively small variations in contact angle suggest that surface chemistry is only slightly modified, while density remains essentially unchanged across all formulations. These results confirm that the observed improvements in mechanical properties are not related to macroscopic changes in material composition or packing density but instead arise from microstructural rearrangements at the phase boundaries.

Overall, the combined results demonstrate that the efficiency of reactive compatibilizers in recycled multilayer PET systems depends strongly on their chemical functionality and ability to interact with multiple polymer phases simultaneously. EMAGMA emerged as the most effective compatibilizer due to its superior ability to promote interfacial adhesion, reduce phase separation, and enhance energy dissipation mechanisms under mechanical stress. EGMA also provided significant improvements, although to a lesser extent, while EAA was less effective and may even compromise mechanical integrity at higher concentrations.

Although both compatibilizers contain reactive glycidyl methacrylate groups, EMAGMA consistently outperformed EGMA in terms of ductility and impact strength. This behavior may be attributed to the presence of methyl acrylate comonomer, which provides greater chain flexibility while maintaining the reactive epoxy functionality. Consequently, EMAGMA may facilitate a more efficient stress transfer between the heterogeneous phases without compromising the stiffness of the recycled material.

These findings are particularly relevant from a sustainability perspective, as they demonstrate a viable strategy for upgrading post-industrial multilayer PET waste into higher-value recycled materials. Given the increasing volume of multilayer packaging waste and its limited recyclability under conventional processes, the development of efficient reactive compatibilization systems represents a promising route to improve circularity in polymer packaging applications, improving the mechanical, thermal, and morphological properties of recycled multilayer polyethylene terephthalate (mPET).

4. Materials and Methods

4.1. Materials

The recycled feedstock used in this study consisted of post-industrial multilayer food-packaging scraps supplied by an industrial packaging manufacturer. The multilayer structure was known to contain polyethylene terephthalate (PET), polyethylene (PE), and ethylene vinyl alcohol (EVOH) layers. However, the supplier did not disclose the relative weight fraction or thickness of each layer. Consequently, the material was

treated as a real industrial multilayer waste stream rather than as a model blend with controlled composition.

The compatibilizers evaluated in this work were poly(ethylene-co-acrylic acid) (EAA, 5 wt.% acrylic acid), poly(ethylene-alt-maleic anhydride) (EMA, average Mw 100,000–500,000 g mol^{-1}, powder), poly(ethylene-co-glycidyl methacrylate) (EGMA, pellets, containing 8 wt.% glycidyl methacrylate, melt index 5 g/10 min at 190 °C/2.16 kg), poly(ethylene-co-methyl acrylate-co-glycidyl methacrylate) (EMAGMA, pellets, containing 8 wt.% glycidyl methacrylate and 25 wt.% methyl acrylate, melt index 6 g/10 min at 190 °C/2.16 kg), and maleic anhydride (MA). All compatibilizers were supplied by Sigma-Aldrich (St. Louis, MO, USA) and used as received without further purification. The selected commercial compatibilizers contain different reactive functional groups, including carboxylic acid, anhydride, and epoxy moieties, with different functional group contents depending on the commercial product. The chemical structure of the compatibilizers can be seen in Figure 16. These functionalities can promote interfacial adhesion and reactive compatibilization between immiscible polymer phases commonly found in multilayer packaging waste, thereby improving blend morphology and mechanical performance.

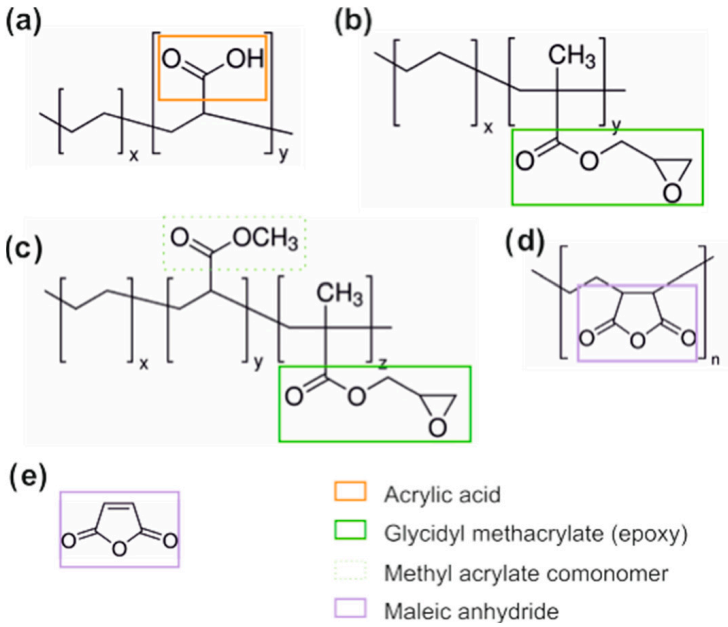


Figure 16. Chemical structures and main reactive functional groups of the commercial compatibilizers used in this study: (**a**) poly(ethylene-co-acrylic acid) (EAA); (**b**) poly(ethylene-co-glycidyl methacrylate) (EGMA); (**c**) poly(ethylene-co-methyl acrylate-co-glycidyl methacrylate) (EMAGMA); (**d**) poly(ethylene-alt-maleic anhydride) (EMA); (**e**) maleic anhydride (MA). The highlighted functional moieties correspond to the reactive sites reported in the literature to participate in the proposed compatibilization mechanisms discussed in Section 4.1.

4.2. Characterization of the Post-Industrial Multilayer PET Feedstock

The recycled material consisted of post-industrial multilayer PET edge trims generated during the manufacture of rigid food packaging. Owing to the industrial origin of the waste, the exact composition and relative proportion of the different polymeric layers were not available. The material was primarily composed of PET together with polyolefin-based layers and adhesive tie layers, resulting in a heterogeneous multilayer structure. Therefore, a preliminary characterization of the residue was carried out to determine its particle size distribution, bulk density, and moisture content prior to processing.

4.2.1. Particle Size Distribution of the mPET Flakes

The determination of particle size and size distribution was carried out in accordance with UNE-EN 15348:2024. The test was performed using a RP200N Electromagnetic Sieve Shaker (Cisa, Barcelona, Spain). Sieves with square mesh openings of 1, 2, 3.15, 4, 6.30, 8, and 12.5 mm were used. A 150 g sample was sieved for 12 min using a vibrating sieve shaker. The test was performed in duplicate.

4.2.2. Determination of Bulk Density

The bulk density of the mPET flake residue was determined in accordance with UNE-EN ISO 60:2000. A calibrated measuring vessel was filled by free pouring of the material without compaction or vibration (Coesfel GmbH & Co., kG, Dortmund, Germany). After leveling the surface, the mass of the material contained in the vessel was measured, and the bulk density was calculated as the mass-to-volume ratio. The test was performed in duplicate, and the average value was reported.

4.2.3. Determination of Moisture Content

The moisture content (MC) of the multilayer mPET flakes was determined gravimetrically by measuring the weight loss after oven drying. Approximately 11–12 g of flakes were weighed (I_w) and dried in a convection oven at 105 °C for 24 h. After drying, the samples were cooled to room temperature in a desiccator and weighed again (F_w). The moisture content was calculated according to Equation (1):

$$MC(\%) = \frac{I_w - F_w}{I_w} \times 100 \quad (1)$$

where I_w is the initial sample weight before drying and F_w is the final sample weight after oven drying.

The moisture determination was carried out at 105 °C in accordance with the standard procedure to ensure complete water removal and accurate gravimetric quantification. This analytical procedure should not be confused with the drying conditions adopted prior to extrusion (40 °C, 24 h), which were selected to preserve the morphology of the multilayer flakes and avoid physical deformation of the material.

4.3. Formulation Development

To improve the recyclability and performance of the recycled multilayer PET (mPET), different reactive compatibilization strategies were evaluated by incorporating the selected compatibilizers at concentrations ranging from 1 to 5 parts per hundred resin (phr). The compositions of the developed formulations and their corresponding injection-molding behavior are summarized in Table 7.

The compatibilizer content (1–5 phr) was selected based on dosage ranges commonly employed for commercial reactive compatibilizers in mechanical recycling and polymer blend compatibilization. Accordingly, the investigated formulations were designed to compare the practical performance of commercially available compatibilizers under equivalent industrial processing conditions rather than to optimize the concentration of a specific additive or normalize their efficiency according to the concentration of reactive functional groups. From an industrial perspective, the selection of compatibilizer content cannot be based exclusively on mechanical performance but must also consider the additional cost of incorporating the compatibilizer. Therefore, concentrations above 5 phr were not included in the present study, as they may reduce the economic competitiveness of recycled materials despite the possibility of achieving further improvements in mechanical performance.

Table 7. Composition of the developed formulations and their injection-molding behavior.

Sample	Compatibilizer Content (phr *)	Injection Behavior
mPET	-	Correct
mPET EAA_3	3 EAA	Correct
mPET EAA_5	5 EAA	Correct
mPET EMA_3	3 EMA	Incomplete
mPET EMA_5	5 EMA	Incomplete
mPET EGMA_1	1 EGMA	Correct
mPET EGMA_2	2 EGMA	Correct
mPET EGMA_3	3 EGMA	Correct
mPET EGMA_4	4 EGMA	Correct
mPET EGMA_5	5 EGMA	Correct
mPET EMAGMA_1	1 EMAGMA	Correct
mPET EMAGMA_2	2 EMAGMA	Correct
mPET EMAGMA_3	3 EMAGMA	Correct
mPET EMAGMA_4	4 EMAGMA	Correct
mPET MA_3	3 MA	Incomplete
mPET MA_5	5 MA	Incomplete

* phr: parts per hundred resin.

4.4. Sample Preparation and Processing

Prior to extrusion, the recycled multilayer flakes were dried at 40 °C for 24 h. This moderate drying temperature was selected to minimize physical changes in the heterogeneous multilayer feedstock before processing. Preliminary observations showed that drying at 105 °C caused slight curvature of the flakes and partial adhesion between particles, whereas drying at 40 °C preserved the original morphology. Furthermore, no processing defects associated with residual moisture, such as bubble formation, vapor evolution or unstable melt flow, were observed during extrusion or injection molding. After the drying stage, the corresponding formulations were prepared according to the compositions described in Table 7.

Each formulation was compounded using an Xplore MC 15 HT co-rotating twin-screw extruder (Xplore Instruments BV, Sittard, The Netherlands) at a processing temperature of 260 °C and a screw speed of 100 rpm. After introducing the materials into the extruder, a residence time of 1 min was allowed before extrusion to promote melt homogenization and facilitate the interaction between the recycled matrix and the compatibilizers.

The compounded materials were subsequently injection molded using an Xplore IM 12 microinjection molding machine (Xplore Instruments BV, Sittard, The Netherlands). The injection process was carried out at an injection temperature of 260 °C, a mold temperature of 70 °C, and an injection pressure of 14 bar.

Standardized specimens were produced for the subsequent mechanical characterization tests. The corresponding specimen geometries and testing standards are described in the respective characterization sections.

4.5. Sample Injectability

Preliminary injection-molding trials were carried out as a screening step to evaluate the processability of the different compatibilizers under identical processing conditions. Compatibilizers that did not produce defect-free specimens under these fixed conditions were discarded from the subsequent study.

The formulations containing EMA at both investigated concentrations (3 and 5 phr) and MA at 3 and 5 phr exhibited incomplete mold filling and did not allow the production of defect-free specimens suitable for subsequent characterization. Representative examples of these defective specimens are shown in Figure 17.

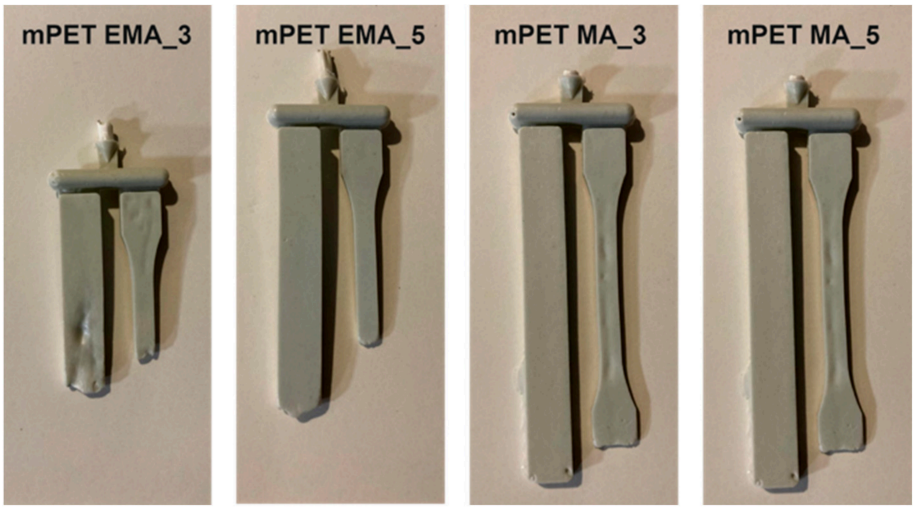


Figure 17. Representative injection-molded specimens obtained from EMA- and MA-containing formulations showing incomplete mold filling and processing defects.

In contrast, the formulations containing EGMA and EMAGMA at all investigated concentrations were successfully molded, producing specimens with complete mold filling and adequate dimensional stability.

The observed differences in injectability indicate that the compatibilizers significantly influenced the processing behavior of the recycled multilayer material. Since rheological characterization was not included in the experimental design, the specific mechanisms responsible for the observed differences in processability cannot be conclusively established. Therefore, no mechanistic interpretation regarding the origin of these processing limitations is proposed in the present work.

Based on the injection-molding trials, only the formulations exhibiting acceptable processability under the selected processing conditions were selected for subsequent characterization. Consequently, the formulations containing EAA, EGMA, and EMAGMA, together with the unmodified mPET reference, were subjected to mechanical, thermal, morphological, and surface characterization. The EMA- and MA-containing formulations were excluded because defect-free specimens suitable for characterization could not be obtained under the selected injection-molding conditions.

4.6. Mechanical Characterization

4.6.1. Tensile Testing

Tensile tests were carried out according to the ISO 527-1:2019 standard using an ELIB 30 universal testing machine manufactured by S.A.E. Ibertest (Madrid, Spain) and equipped with a 5 kN load cell. The tests were performed at room temperature using a crosshead speed of 10 mm/min. Microinjected Type 5A specimens were employed and at least five specimens were tested for each formulation, and the average values together with the corresponding standard deviations were calculated. The tensile properties evaluated included maximum tensile strength, Young's modulus, and elongation at break.

4.6.2. Charpy Impact Testing

Impact resistance was evaluated according to ISO 179-1 using a Metrotec PIT-25 Charpy impact tester supplied by Metrotec (San Sebastián, Spain). Prior to testing, the specimens were mechanically notched using a HOYTOM broaching machine (Bilbao, Spain) equipped with a V-type notch geometry and a notch radius of 0.25 mm. The tests were conducted at room temperature using a 6 J pendulum. Six specimens were performed for each formulation, and the mean values together with standard deviations were calculated.

4.6.3. Shore D Hardness

Hardness measurements were performed according to ISO 868 using a Shore D durometer model 673-D supplied by Instruments J. Bot S.A. (Barcelona, Spain). Six measurements were performed at different locations on the specimen after a stabilization time of 15 s. The average hardness values and corresponding standard deviations were subsequently determined.

4.7. Thermal Characterization

4.7.1. Differential Scanning Calorimetry (DSC)

Differential scanning calorimetry (DSC) analyses were performed using a DSC 25 calorimeter (Mettler-Toledo S.A.E., Barcelona, Spain) under a nitrogen atmosphere. Samples (5–6.5 mg) were sealed in aluminum pans and subjected to a thermal cycle consisting of heating from 30 to 270 °C, cooling to 30 °C, and a second heating scan to 350 °C, all at 10 °C min^{-1}. Thermal transitions were determined from the second heating run to eliminate the effects of previous thermal history. DSC was used to evaluate the thermal behavior of the developed formulations, focusing on the identification of melting transitions and changes in melting enthalpy.

4.7.2. Thermogravimetric Analysis (TGA)

The main thermal degradation parameters, including the onset degradation temperature (T_{onset}) and the temperature corresponding to the maximum degradation rate (T_{max}), were determined by thermogravimetric analysis (TGA) using a Q500 thermogravimetric analyzer (TA Instruments, New Castle, DE, USA). Samples weighing between 8 and 10 mg were placed in 70 µL alumina crucibles. The samples were subjected to the following temperature program: heating from 30 to 600 °C under a nitrogen (N_2) atmosphere at a rate of 10 °C min^{-1}, followed by heating from 600 to 1000 °C under an oxygen (O_2) atmosphere at the same heating rate (10 °C min^{-1}) using a purge gas flow of 10 mL min^{-1}. All analyses were performed in triplicate. TGA was used to evaluate the thermal stability of the developed formulations by determining the onset degradation temperature (T_{onset}) and the temperature of the maximum degradation rate (T_{max}).

4.8. FTIR Analysis

The functional groups present in the recycled materials and compatibilized formulations were analyzed by Fourier transform infrared spectroscopy with attenuated total reflectance (FTIR-ATR) using a PerkinElmer Spectrum Two spectrometer. The analyses were performed according to ISO 10640:2011. Spectra were collected in ATR mode over a wavenumber range between 4000 and 400 cm^{-1} using a resolution of 4 cm^{-1} and averaging 10 scans per sample.

4.9. Contact Angle Measurements

Surface wettability was evaluated through static water contact angle measurements using an EasyDrop Standard contact angle goniometer (model FM140, KRÜSS GmbH, Hamburg, Germany). The equipment consisted of a sample stage, a liquid dosing syringe system, a high-resolution camera, and a diffuse illumination source. Deionized water was used as the test liquid, and five measurements were performed for each sample at different locations on the surface. The contact angle measurements were used to evaluate the influence of the compatibilizers on the surface wettability and hydrophobic character of the recycled formulations. The reported values correspond to the average of the five replicates.

4.10. Density Measurements

Density measurements were performed using a Sartorius Entris hydrostatic balance (Göttingen, Germany) according to the Archimedes methodperfec, which allows for the measurement of a solid object in both air and water. The density of each formulation was determined by measuring the specimen weight in air and in distilled water. The density values were calculated according to Equation (2).

At least five measurements were performed for each formulation, and the average values together with the corresponding standard deviations were calculated.

$$\rho = \frac{W(a) \cdot \rho(fl)}{W(a) - W(fl)} \quad (2)$$

where ρ is the density of the solid body, $\rho(fl)$ is the density of the liquid, $W(a)$ is the weight of the solid body in air, and $W(fl)$ is the weight of the solid body in the liquid.

4.11. Microscopic Characterization

Field emission scanning electron microscopy (FESEM) was performed using a ZEISS ULTRA microscope (Oxford Instruments, Oxfordshire, UK) to investigate the fracture surface morphology of the recycled multilayer PET and compatibilized formulations. Representative micrographs were acquired at different magnifications under an accelerating voltage of 1.5 kV. The analyzed specimens corresponded to impact-fractured samples, whose fracture surfaces were sputter-coated with a thin platinum layer using a Leica Microsystems EM MED0200 high-vacuum sputter coater (Buffalo Grove, IL, USA) to improve electrical conductivity and image quality.

To quantitatively evaluate the compatibilization effect, representative FESEM micrographs acquired at 1000× magnification were analyzed using Fiji (ImageJ version 1.54p, National Institutes of Health, Bethesda, MD, USA). Only dispersed domains that remained embedded in the polymer matrix after fracture, were approximately circular, completely visible within the image, and did not intersect the image borders were considered. Pull-out cavities and irregular fractured regions were excluded from the analysis. The equivalent circular diameter (ECD) of each dispersed domain was calculated from the measured projected area according to Equation (3). Between 36 and 64 dispersed domains were analyzed for each representative formulation. Statistical analysis was performed using one-way analysis of variance (ANOVA), followed by Tukey's multiple comparison test at a confidence level of 95% ($p < 0.05$).

$$ECD = \sqrt{\frac{4 \cdot A}{\pi}} \quad (3)$$

where A is the projected area of the dispersed domain.

5. Conclusions

The present study demonstrates that the incorporation of reactive compatibilizers is an effective strategy for improving the mechanical, thermal, and morphological properties of recycled multilayer polyethylene terephthalate (mPET). The recycling of multilayer packaging materials remains a major challenge due to the immiscibility between the different polymer phases present in these structures, such as PET and polyethylene-based materials. As observed throughout this work, the appropriate selection of compatibilizers can significantly improve phase dispersion and the overall performance of the recycled material, facilitating the production of recycled materials with enhanced structural integrity and mechanical performance.

Among the compatibilizers evaluated, ethylene-glycidyl methacrylate (EGMA) and ethylene-methyl acrylate-glycidyl methacrylate (EMAGMA) exhibited the best overall performance. Both compatibilizers produced substantial improvements in ductility and impact resistance while maintaining acceptable tensile strength and hardness values. In particular, formulations containing EMAGMA showed the highest elongation at break and impact strength values, demonstrating a strong toughening effect. The formulation containing 3 phr EMAGMA reached an elongation at break of 194%, while the impact strength of EMAGMA_5 increased by approximately 100% compared to the reference mPET. These results highlight the effectiveness of EMAGMA as a compatibilization strategy for improving the mechanical performance of recycled multilayer PET systems.

Analyzing the overall correlation between the tensile and impact strength properties, a clear relationship between ductility and toughness was observed. Materials with higher elongation at break generally exhibited improved impact strength, confirming that increased ductility enhances the ability of the material to absorb and dissipate impact energy. In this context, EMAGMA proved to be the most effective modifier for improving toughness, as it significantly increased both elongation at break and impact resistance while still maintaining acceptable hardness values. EGMA also demonstrated a significant improvement in impact resistance and ductility, providing a balanced combination of toughness and mechanical strength. The superior performance of EGMA and EMAGMA was consistent with the more homogeneous morphologies observed by FESEM, suggesting improved phase dispersion within the heterogeneous recycled multilayer structure.

In contrast, the incorporation of ethylene-acrylic acid (EAA) produced only moderate improvements in flexibility and did not significantly enhance the impact resistance. Although the addition of 3 phr EAA increased the elongation at break, higher concentrations resulted in a reduction in both tensile strength and ductility, suggesting limited compatibilization efficiency. Furthermore, formulations containing ethylene-alt-maleic anhydride (EMA) and maleic anhydride (MA) exhibited severe processing difficulties and could not be properly injection molded. These results highlight the importance of compatibilizer chemistry in determining both processability and final material performance.

The DSC analyses showed that all compatibilized formulations exhibited higher PET melting enthalpy (ΔH_m) values than the reference mPET, indicating that the reactive compatibilizers modified the crystalline organization of the PET-rich phase to different extents. However, these thermal changes did not directly correlate with the mechanical performance of the materials, highlighting that improved tensile ductility and impact resistance are primarily associated with enhanced interfacial compatibilization rather than with changes in PET melting enthalpy alone. TGA confirmed that the incorporation of EAA, EGMA, and EMAGMA preserved the thermal stability of the recycled multilayer material. FTIR analyses confirmed the heterogeneous composition of the recycled multilayer material, revealing the coexistence of polyester and polyethylene phases, while FESEM observations demonstrated clear morphological differences among the investigated formulations. In particular, the EGMA- and EMAGMA-containing formulations exhibited a more homogeneous phase distribution and fewer large interfacial defects than the reference mPET and the EAA-containing systems, consistent with their superior mechanical performance.

Overall, the results obtained in this work confirm that reactive compatibilization represents a promising route for the valorization of recycled multilayer PET waste streams within a circular economy framework. The use of suitable compatibilizers allows for the transformation of low-value multilayer plastic waste into recycled materials with improved toughness, flexibility, and structural performance, expanding their potential applications in industrial sectors requiring high-performance recycled polymers.

Author Contributions: Conceptualization, A.I.-G., A.M.-G. and M.D.S.; Methodology, A.U.G., F.G.P. and A.I.-G.; Software, A.U.G., F.G.P., A.I.-G. and M.D.S.; Validation, A.U.G., F.G.P. and M.D.S.; Formal analysis, A.U.G. and M.D.S.; Investigation, A.U.G. and A.I.-G.; Resources, A.I.-G., A.M.-G. and M.D.S.; Data curation, F.G.P.; Writing—original draft preparation, A.U.G.; Writing—review and editing, A.I.-G., A.M.-G. and M.D.S.; Visualization, A.U.G., A.I.-G. and M.D.S.; Supervision, M.D.S.; Project administration, A.M.-G. and M.D.S.; Funding acquisition, A.M.-G. and M.D.S. All authors have read and agreed to the published version of the manuscript.

Funding: This research was funded by the European Union through the Horizon Europe program (HORIZON-CL6-2023-CIRCBIO-02) under the CIRCSYST project (Grant Agreement No. 101135505).

Data Availability Statement: The raw data supporting the conclusions of this article will be made available by the authors on request.

Acknowledgments: The authors would like to thank the CIRCSYST project consortium for their valuable collaboration.

Conflicts of Interest: The authors declare no conflict of interest.

References

1. Bauer, A.-S.; Tacker, M.; Uysal-Unalan, I.; Cruz, R.M.; Varzakas, T.; Krauter, V. Recyclability and redesign challenges in multilayer flexible food packaging—A review. *Foods* **2021**, *10*, 2702. [CrossRef] [PubMed]
2. Maris, J.; Bourdon, S.; Brossard, J.-M.; Cauret, L.; Fontaine, L.; Montembault, V. Mechanical recycling: Compatibilization of mixed thermoplastic wastes. *Polym. Degrad. Stab.* **2018**, *147*, 245–266. [CrossRef]
3. Cavuquila, A.; Dias, A.F.; Carreira, G.A.; Portugal, I.; Silva, C.M.; Barros-Timmons, A. Valorization of mixed multilayer plastic waste: An exploratory study. *Waste Manag. Bull.* **2025**, *3*, 100252. [CrossRef]
4. Ügdüler, S.; Van Geem, K.M.; Denolf, R.; Roosen, M.; Mys, N.; Ragaert, K.; De Meester, S. Towards closed-loop recycling of multilayer and coloured PET plastic waste by alkaline hydrolysis. *Green Chem.* **2020**, *22*, 5376–5394. [CrossRef]
5. Walker, T.W.; Frelka, N.; Shen, Z.; Chew, A.K.; Banick, J.; Grey, S.; Kim, M.S.; Dumesic, J.A.; Van Lehn, R.C.; Huber, G.W. Recycling of multilayer plastic packaging materials by solvent-targeted recovery and precipitation. *Sci. Adv.* **2020**, *6*, eaba7599. [CrossRef] [PubMed]
6. Ellis, L.D.; Rorrer, N.A.; Sullivan, K.P.; Otto, M.; McGeehan, J.E.; Román-Leshkov, Y.; Wierckx, N.; Beckham, G.T. Chemical and biological catalysis for plastics recycling and upcycling. *Nat. Catal.* **2021**, *4*, 539–556. [CrossRef]
7. Jehanno, C.; Alty, J.W.; Roosen, M.; De Meester, S.; Dove, A.P.; Chen, E.Y.-X.; Leibfarth, F.A.; Sardon, H. Critical advances and future opportunities in upcycling commodity polymers. *Nature* **2022**, *603*, 803–814. [CrossRef] [PubMed]
8. Amundarain, I.; López-Montenegro, S.; Fulgencio-Medrano, L.; Leivar, J.; Iruskieta, A.; Asueta, A.; Miguel-Fernández, R.; Arnaiz, S.; Pereda-Ayo, B. Improving the Sustainability of Catalytic Glycolysis of Complex PET Waste Through Bio-Solvolysis. *Polymers* **2024**, *16*, 142. [CrossRef] [PubMed]
9. van Vliet, D.M.; Mateman, J.J.; van de Vondervoort, R.H.; Moers, A.P.; Collazo, L.; Mencher, A.; Werten, M.W.; Thiyagarajan, S.; Cordes, A.; Sonnendecker, C. Efficient recycling of PET-PE multilayer packaging materials based on enzymatic depolymerization of PET. *ACS Sustain. Chem. Eng.* **2025**, *13*, 8212–8219. [CrossRef] [PubMed]
10. Moreno, D.D.P.; Saron, C. Influence of compatibilizer on the properties of low-density polyethylene/polyamide 6 blends obtained by mechanical recycling of multilayer film waste. *Waste Manag. Res.* **2018**, *36*, 729–736. [CrossRef] [PubMed]
11. Turriziani, B.B.; Vieira, R.P.; Marangoni Júnior, L.; Alves, R.M.V. Mechanical recycling of multilayer flexible packaging employing maleic anhydride as compatibilizer. *J. Polym. Environ.* **2024**, *32*, 1393–1405.
12. Dagli, S.S.; Kamdar, K.M. Effects of component addition protocol on the reactive compatibilization of HDPE/PET blends. *Polym. Eng. Sci.* **1994**, *34*, 1709–1719. [CrossRef]
13. Kim, S.; Park, C.E.; An, J.H.; Lee, D.; Kim, J. The effect of functional group content on poly (ethylene terephthalate)/high density polyethylene blends compatibilized with poly (ethylene-co-acrylic acid). *Polym. J.* **1997**, *29*, 274–278. [CrossRef]
14. Morshedi Dehaghi, F.; Aberoumand, M.; Sundararaj, U. A promising recycling strategy via processing polypropylene/recycled poly (ethylene terephthalate): Reactive extrusion using dual compatibilizers. *Polymers* **2024**, *16*, 2439. [CrossRef] [PubMed]
15. Uehara, G.A.; França, M.P.; Canevarolo, S.V. Recycling assessment of multilayer flexible packaging films using design of experiments. *Polímeros* **2015**, *25*, 371–381. [CrossRef]

16. de Sousa Filho, V.A.; de Alencar Lira, M.C.; Bonfim, R.L.P.; da Cunha, R.B.; Cavalcanti, S.N.; Brito, L.B.Q.; Agrawal, P.; de Figueiredo Brito, G.; de Mélo, T.J.A. Reactive and non-reactive compatibilization of polyethylene terephthalate glycol/thermoplastic polyurethane (PETG/TPU) blends for 3D/4D printing applications. *React. Funct. Polym.* **2025**, *215*, 106393. [CrossRef]
17. Pawlak, A.; Morawiec, J.; Pazzagli, F.; Pracella, M.; Galeski, A. Recycling of postconsumer poly (ethylene terephthalate) and high-density polyethylene by compatibilized blending. *J. Appl. Polym. Sci.* **2002**, *86*, 1473–1485. [CrossRef]
18. Coba-Daza, S.; Otaegi, I.; Aramburu, N.; Guerrica-Echevarria, G.; Irusta, L.; González, A.; Neubauer, L.; Ramer, G.; Lendl, B.; Hubner, G. Unlocking superior properties in polypropylene/polyethylene terephthalate (PP/PET) blends using an ethylene-butylene-acrylate terpolymer reactive compatibilizer. *Polym. Test.* **2024**, *130*, 108293. [CrossRef]
19. Zervoudakis, A.J.; Sample, C.S.; Peng, X.; Lake, D.; Hillmyer, M.A.; Ellison, C.J. Dihydroxy polyethylene additives for compatibilization and mechanical recycling of polyethylene terephthalate/polyethylene mixed plastic waste. *ACS Macro Lett.* **2022**, *11*, 1396–1402. [CrossRef] [PubMed]
20. Ronkay, F. Influence of short glass fiber reinforcement on the morphology development and mechanical properties of PET/HDPE blends. *Polym. Compos.* **2011**, *32*, 586–595. [CrossRef]
21. Tang, X.; Liu, C.; Keum, J.; Chen, J.; Dial, B.E.; Wang, Y.; Tsai, W.-Y.; Bras, W.; Saito, T.; Bowland, C.C. Upcycling of semicrystalline polymers by compatibilization: Mechanism and location of compatibilizers. *RSC Adv.* **2022**, *12*, 10886–10894. [CrossRef] [PubMed]
22. Taghavi, S.K.; Shahrajabian, H.; Hosseini, H.M. Detailed comparison of compatibilizers MAPE and SEBS-g-MA on the mechanical/thermal properties, and morphology in ternary blend of recycled PET/HDPE/MAPE and recycled PET/HDPE/SEBS-g-MA. *J. Elastomers Plast.* **2018**, *50*, 13–35. [CrossRef]
23. Dobrovszky, K.; Ronkay, F. Effects of SEBS-g-MA on rheology, morphology and mechanical properties of PET/HDPE blends. *Int. Polym. Process.* **2015**, *30*, 91–99. [CrossRef]

Disclaimer/Publisher's Note: The statements, opinions and data contained in all publications are solely those of the individual author(s) and contributor(s) and not of MDPI and/or the editor(s). MDPI and/or the editor(s) disclaim responsibility for any injury to people or property resulting from any ideas, methods, instructions or products referred to in the content.